Seasonal changes in plankton respiration and bacterial metabolism in a temperate Shelf Sea.

E. Elena García-Martín[1*], Chris J. Daniels[2], Keith Davidson[3], Clare E. Davis[4], Claire Mahaffey[4], Kyle M.J. Mayers[2,5], Sharon McNeill[3], Alex J. Poulton[2,6], Duncan A. Purdie[5], Glen A. Tarran[7], Carol Robinson[1]

[1] Centre for Ocean and Atmospheric Sciences, School of Environmental Sciences, University of East Anglia, Norwich Research Park, Norwich, NR4 7TJ, UK

[2]Ocean Biogeochemistry and Ecosystems, National Oceanography Centre, Waterfront Campus, European Way, Southampton SO14 3ZH, UK

[3]Scottish Association for Marine Science, Scottish Marine Institute, Oban, Argyll, PA371QA, Scotland, UK

[4]Department of Earth, Ocean, and Ecological Sciences, University of Liverpool, Liverpool, L69 3GP, UK

[5]Ocean and Earth Science, University of Southampton, National Oceanography Centre Southampton, Southampton, SO14 3ZH, UK

[6]The Lyell Centre, Heriot-Watt University, Edinburgh, EH14 4AS, UK

[7]Plymouth Marine Laboratory, Prospect Place, Plymouth, PL1 3DH, UK

[*] Corresponding author: Centre for Ocean and Atmospheric Sciences, School of Environmental Sciences, University of East Anglia, Norwich Research Park, Norwich, NR4 7TJ, UK

Email address: Enma.Garcia-Martin@uea.ac.uk. Tel: 0044 (0)1603 593162

Abstract

Seasonal variability between November 2014, April 2015 and July 2015 in plankton respiration and bacterial metabolism is reported for the upper and bottom mixing layers at two stations in the Celtic Sea, UK. Depth- integrated microplankton community respiration (considered as the respiration of plankton < 5 mm) (CR_{O2}) within the upper mixing layer showed strong seasonal changes with maximum values in April (169 ± 5 mmol O_2 m^{-2} d^{-1}) and a minima in November (27 ± 5 mmol O_2 m^{-2} d^{-1}). Rates of respiration and (gross) primary production rates (^{14}C-PP) showed different seasonal variability, resulting in seasonal changes in ^{14}C-PP:CR_{O2} ratios. In April, the system was net autotrophic (^{14}C-PP:CR_{O2} > 1), with a surplus of organic matter available for export, while in July balanced metabolism occurred (^{14}C-PP:CR_{O2} = 1) due to an increase in microplankton respiration and a decrease in (gross) primary production. Changes in microplankton respiration were mainly driven by changes in the respiration of the >0.8 µm size fraction. Monthly average upper mixing layer depth-integrated heterotrophic bacterial respiration rates (considered to be the respiration measured in the 0.2-0.8 µm size fraction) were similar in November and April (27 ± 2 and 28 ± 3 mmol O_2 m^{-2} d^{-1}, respectively) and lowest in July (13 ± 2 mmol O_2 m^{-2} d^{-1}). The percentage of microplankton respiration attributable to bacteria was higher in November (38 ± 2 %) than in April (26 ± 3 %) or July (20 ± 2 %). Bacterial production also showed a strong seasonality, with maximum values in July (16.6 ± 0.3 mmol C m^{-2} d^{-1}) and minima in November (4.3 ±0.1 mmol C m^{-2} d^{-1}). The greater variability in bacterial production compared to bacterial respiration drove seasonal changes in bacterial growth efficiencies, which had maximum values of 71 ± 4% in July and minimum values of 18 ± 2% in November. The observed seasonality in microplankton community respiration and bacterial metabolism were best described in distance-based redundancy analysis by a combination of temperature, nitrate+nitrite, silicate and ammonium concentrations, each having a different

relative importance in the different months. Interestingly, changes in bacterial carbon demand were independent of the amount of dissolved organic carbon produced by phytoplankton.

Microplankton community respiration and bacterial production were higher in the upper mixing layers than in the bottom mixing layers (between 3 and 9-fold for microplankton community respiration and 3 and 7-fold for bacterial production) in November, April and July. However, the rates of bacterial respiration were not statistically different (paired t-test, $p > 0.05$) between the two mixing layers in any of the three sampled seasons. These results highlight that, contrary to previous results in Shelf seas, the production of CO_2 by the microplankton community in upper mixing waters, which is then available to degas to the atmosphere, is greater than the respiratory production of dissolved inorganic carbon in deeper waters, which contributes to offshore export.

Keywords: plankton community respiration; bacterial production; bacterial respiration; bacterial growth efficiency; dissolved organic carbon; upper / bottom mixing layers; shelf sea.

Introduction

Shelf seas are regions of significant primary production and carbon export from continental areas to the deep ocean (Thomas et al. 2004, Carlson et al. 2010). Particulate and dissolved organic carbon is synthesized in the upper surface layers by plankton, as well as being introduced from continental runoff and atmospheric deposition. Once in the upper mixing layer, organic carbon can be consumed, transformed, or transported to depth. The amount of organic carbon annually exported from the upper mixing layer depends on the efficiency of remineralization in the upper mixing layer. Between 1 % and 40 % of primary production is exported from the euphotic layer (Herndl and Reinthaler 2013), with less than 5 % ultimately buried in shelf sea sediments (de Haas et al. 2002). This implies high rates of respiration also occur below the surface mixing layer (Thomas et al. 2004). Despite their importance in the degradation of organic matter, and therefore export, the magnitude and variability of plankton and bacterial respiration is much less well understood than that of phytoplankton production in coastal and shelf seas.

The Celtic Sea is a north western European shelf sea characterized by winter vertical mixing, reduced vertical mixing in spring associated with an increase in phytoplankton abundance, and thermal stratification in summer (Pingree 1980, Joint et al. 1986). The Celtic Sea has been the subject of several physical and biogeochemical studies. The most extensive was conducted by Joint et al. (2001) and focused on plankton activity, measuring pelagic primary production, bacterial production, microzooplankton respiration and potential sedimentation. Since then, several studies have described the physicochemical characteristics that regulate primary production in stratified waters (Hickman et al. 2012), photoacclimation and photoadaptation by phytoplankton (Moore et al. 2006), the distribution and survival of plankton in the thermocline (Sharples 2001), and the effect of resuspension of nutrients from

sediments on the abundance and productivity of phytoplankton and bacteria (Davidson et al. 2013).

However, despite the importance of plankton respiration and bacterial growth efficiencies (BGE, defined as bacterial production divided by the sum of bacterial production and bacterial respiration) to the transfer of organic carbon produced by phytoplankton to deeper waters (Legendre et al. 2015), plankton community respiration was not measured in any of the former studies in this region. In fact, there are relatively few studies which determine the seasonal variability in plankton community respiration and bacterial growth efficiencies in temperate shelf seas (Blight, et al. 1995, Serret et al. 1999, Arbones et al. 2008). These seasonal studies reported peaks in plankton community respiration in spring and summer, associated with higher phytoplankton production (Blight, et al. 1995, Serret et al. 1999, Arbones et al. 2008). The close coupling between primary production and respiration implies that the synthesis of organic matter by the phytoplankton is linked with higher phytoplankton respiration and / or stimulates heterotrophic plankton community (Blight et al. 1995) and bacterial respiration (Lemée et al. 2002). The newly produced organic matter also enhances bacterial production which drives an increase in BGE (Lemée et al. 2002, Reinthaler and Herndl 2005).

The relative magnitude of primary production, plankton respiration and bacterial growth efficiency in the upper and bottom mixing layers of shelf seas determines the efficiency of export from the surface layers, and potential sequestration to the sediment or transfer off shelf. These metabolic processes are influenced by environmental conditions such as temperature and the availability of dissolved inorganic and organic nutrients (Elser et al. 1995, López-Urrutia and Morán 2007, Lee et al. 2009, Kritzberg et al. 2010), but there is no clear consensus as to which environmental factors most influence the individual processes in natural waters.

The aim of this study was to quantify any difference in microplankton community respiration (considered as the respiration of plankton smaller than 5 mm), bacterial respiration and bacterial production rates between the upper and bottom mixing layers of the Celtic Sea, and to assess how environmental and biological conditions (temperature, nutrient concentration, chlorophyll-*a* concentration) influence microplankton respiration, bacterial metabolism and bacterial growth efficiency. Data from a central shelf station were compared with data from a station close to the shelf edge to assess the potential influence of different ocean dynamics on microplankton community respiration and bacterial metabolism.

Material and Methods

2.1 Study site and sampling procedure

Water samples were collected during three cruises in the Celtic Sea as part of the UK Shelf Sea Biogeochemistry program (see Sharples et al., this issue). This study was conducted at two stations: one at the Central Celtic Sea (CCS, 49.39 ºN latitude, 8.58 ºW longitude), with a maximum depth of 143 m, and another at the Shelf Edge (CS2), a station with a maximum depth of 200 m and situated on the shelf edge (48.57 ºN latitude, 9.5 ºW longitude) (see Figure in Sharples et al., this issue). CCS was sampled on 4 days in November 2014 (10^{th}, 12^{th}, 22^{nd}, 25^{th}), on 6 days in April 2015 (4^{th}, 6^{th}, 11^{th}, 15^{th}, 20^{th}, 25^{th}) and on 3 days in July 2015 (14^{th}, 24^{th}, 29^{th}). CS2 was sampled on 2 occasions in November 2014 (18^{th}, 20^{th}), 2 occasions in April 2015 (10^{th}, 24^{th}) and once during July 2015 (19^{th}). At each station water samples were collected pre-dawn (~01:00 – 04:00 GMT) from 7 depths with 20-L Niskin bottles mounted on a sampling rosette to which was attached a conductivity-temperature-depth profiler (Sea-Bird Electronics, Washington, USA). Six of these sample depths were in the upper mixing layer (UML) at 60%, 40%, 20%, 10%, 5% and 1% of surface irradiance (I_0)

(see Poulton et al., this issue). Light sampling depths were estimated by back calculation of the vertical attenuation coefficient of PAR (Kd, m^{-1}) based on either (a) assuming that the base of the thermocline was at or close to the 1% I_0 (November, April), or (b) that the sub-surface chlorophyll-a maximum was at or close to a depth of 5% I_0 (July) (see Hickman et al., 2012, Poulton et al., this issue). The other sample depth was at 10-20 m below the base of the thermocline and within the bottom mixing layer (BML) at irradiances <0.1 % I_0. The horizon between the UML and the BML was identified by the depth of the base of the thermocline (Fig. 1). Sea water was carefully decanted from the Niskin bottles into 10 L carboys for subsequent determination of microplankton community respiration derived from both dissolved oxygen consumption and the reduction of 2-(ρ-iodophenyl)-3-(ρ-nitrophenyl)-5phenyl tetrazolium chloride (INT). Water samples for the determination of chlorophyll-*a* (Chl-*a*), (gross) primary production (^{14}C-PP), phytoplankton production of dissolved organic carbon (*p*DOC), bacterial production (BP) and bacterial abundance (BA) were also taken, when possible, from the same Niskin bottles as the samples collected for the determination of microplankton community respiration. Water samples for determination of dissolved organic carbon (DOC) and nitrogen (DON) were collected at the same time and from the same depths, but from an adjacent Niskin bottles. The full sampling procedure for the determination of nutrients and Chl-*a* concentration can be found in Hickman et al. (this issue), for bacterial abundance in Tarran et al. (this issue), and for the concentration of DOC and DON in Davis et al. (this issue). A summary of the sampling and analytical protocol is also reported here.

2.2 Nutrients, total chlorophyll *a* and bacterial abundance

Nitrate+nitrite, ammonium, phosphate and silicate concentrations were determined using a Bran & Luebbe AAIII segmented flow colourimetric autoanalyser (Brewer and Riley 1965,

Grasshoff 1976, Kirkwood 1989). Water samples were collected directly from the Niskin bottles at each station and analysed within 1-2 hours of sampling.

Samples for total Chl-*a* were collected from the UML by filtering 200-250 mL of sea water through 25 mm diameter Fisherbrand MF300 or Whatman GF/F filters (effective pore size for both 0.7 μm). After filtration, pigments were extracted in 90 % acetone for 18-20 h in the dark at 4 ˚C. Chlorophyll-*a* concentration was determined fluorometrically on a Turner Trilogy fluorometer calibrated against a pure Chl-*a* extract (Sigma) (see also Hickman et al., this issue).

Samples for the enumeration of heterotrophic bacteria were collected from the Niskin bottles into clean 250 mL polycarbonate bottles. Subsamples were then pipetted into 2 mL microcentrifuge tubes and fixed with glutaraldehyde (50%, TEM grade, 0.5% final concentration) within 30 minutes of collection. After fixing for 30 min at 4 ˚C, samples were stained with SYBR Green I DNA dye (Invitrogen) for 1 h at room temperature in the dark and analysed immediately for bacterial abundance (BA) by flow cytometry (Tarran et al., this issue).

2.3 Dissolved organic carbon and total dissolved nitrogen

Sea water samples for measurement of dissolved organic carbon (DOC) and total dissolved nitrogen (TDN) were collected from between 3 and 5 sampling depths which corresponded to those sampled for microplankton community respiration, as detailed below. Samples were filtered through pre-combusted (450 ˚C) GF/F filters (Whatman, nominal pore size 0.7 μm) under low vacuum pressure (< 10 mmHg) and preserved with 20 μL of 50 % (v/v) hydrochloric acid. Samples were analysed onshore using high temperature catalytic oxidation (HTCO) on a Shimadzu TOC-V_{CPN}. The limits of detection for DOC and TDN were 3.4 μmol L^{-1} and 1.8 μmol L^{-1} respectively, with a precision of 2.5 %. Consensus Reference

Materials from the Hansell Laboratory, University of Miami, were analysed daily with a mean and standard deviation for DOC and TDN of 43.9 ± 1.2 µmol L^{-1} (expected range 42 – 45 µmol L^{-1}; n = 39) and 32.9 ± 1.7 µmol L^{-1} (expected range 32.25 – 33.75 µmol L^{-1}), respectively. Concentrations of dissolved organic nitrogen (DON) were determined by subtracting the concentration of inorganic nitrogen (nitrate, nitrite, ammonium) from TDN concentrations (Davies et al., this issue).

2.4 Primary production and production of dissolved organic carbon

The six sampling depths for ^{14}C-PP were all within the UML (five of which corresponded to depths sampled for microplankton community respiration) and *p*DOC was measured at three of these depths. The *p*DOC depths corresponded to the depth at which surface irradiance was attenuated to 60 %, 20 % and 1 % in November and April, and to 60 %, 5 % and 1 % of surface irradiance in July, to account for the potential role of the sub-surface chlorophyll maximum (~5 % surface irradiance; Hickman et al., 2012).

For carbon fixation and *p*DOC, water samples were collected into four 70 mL polycarbonate bottles (3 light, 1 dark), and spiked with 6-11 µCi carbon-14 labelled sodium bicarbonate. The bottles were then incubated in a purpose built constant temperature containerised laboratory at a range of seasonally adjusted irradiance levels using LED light panels and neutral density filters (see Poulton et al., this issue).

On termination of the incubation, a 5 mL sub-sample from the four bottles was filtered through 25 mm 0.2 µm polycarbonate filters, with the filtrates then transferred to 20 mL scintillation vials for the determination of *p*DOC. To remove the dissolved inorganic ^{14}C, 100 µL of 50 % HCl was added to each vial, which were then sealed with a gas-tight rubber septum (Kimble-Kontes) and a centre well (Kimble-Kontes) containing a CO_2 trap

188 (consisting of a Whatman GFA filter soaked with 200 µL β-phenylethylamine). After 12
189 hours, the CO_2 traps were removed and disposed of, and 15 mL of Ultima Gold (Perkin
190 Elmer, UK) liquid scintillation cocktail was added to the filtrate. Spike activity was checked
191 following Mayers et al. (this issue) and activity in the filtrate was determined in a Tri-Carb
192 3100TR Liquid Scintillation Counter. Rates of *p*DOC were determined from these
193 incubations using methods adapted from López-Sandoval et al. (2011) and Poulton et al.
194 (2016).

195 The remaining 65 mL samples from the four bottles were then filtered through 25 mm 0.4 µm
196 polycarbonate filters (Nucleopore™, USA), with extensive rinsing to remove unfixed ^{14}C-
197 labelled sodium bicarbonate and 12 mL of Ultima Gold (Perkin-Elmer, UK) liquid
198 scintillation cocktail added. The activity on the filters was determined using a Tri-Carb
199 3100TR Liquid Scintillation Counter on-board. Daily rates of primary production were scaled
200 up from short-term (6-8 h, dawn to midday) rates of carbon fixation to seasonally adjusted
201 day lengths (9 h November, 14 h April and 16 h July). These daily rates of ^{14}C-PP (see also
202 García-Martín et al., this issue), based on short-term (<8 h) incubations, better approximate
203 "gross" primary production, whilst daily rates presented in companion papers (Mayers et al.,
204 this issue; Poulton et al., this issue; Hickman et al., this issue), based on long-term (24 h)
205 incubations, better approximate "net" primary production (see e.g. Marra, 2002).

206

207 **2.5 Respiration derived from dissolved oxygen consumption**

208 Samples for daily microbial respiration were collected from 5 depths in the UML and one
209 depth in the BML. Daily microplankton community respiration (CR_{O2}) was determined by
210 measuring the decrease in dissolved oxygen after 24 h dark bottle incubations. Dissolved
211 oxygen concentration was measured by automated Winkler titration performed with a

Metrohm 765 burette to a photometric end point (Carritt and Carpenter 1966). Ten gravimetrically calibrated 60 mL borosilicate glass bottles were carefully filled with seawater from each 10 L carboy. Water was allowed to overflow during the filling, and care was taken to prevent bubble formation in the silicone tube. Five bottles were fixed at the start of the incubation ("zero") with 0.5 mL of 3 M manganese sulphate and 0.5 mL of 4 M sodium iodide/8 M sodium hydroxide solution (Carritt and Carpenter 1966). The other five bottles were placed underwater in darkened temperature controlled incubators located in a temperature controlled room for 24 hours ("dark"). The incubation temperatures were ±1.0 °C of the in situ temperature. Bottles were removed from the incubators after 24 hours and the samples fixed as described for the "zero" bottles above. All bottles were analysed together within the next 24 hours. Daily microplankton community respiration was calculated from the difference in oxygen concentration between the mean ± standard error (±SE) of the replicate "zero" measurements and the mean ±SE of the replicate "dark" measurements, and is reported with ± SE. Microplankton community respiration in moles of C was calculated from the CR_{O2} rates by applying a respiratory quotient of 1.

2.6 Respiration derived from INT reduction

Samples for respiration derived from INT reduction were collected from the same 6 depths as for CR_{O2}. Five 200 mL dark glass bottles were filled with seawater from each 10 L carboy. The samples in two of these bottles were immediately fixed by adding formaldehyde (2% w/v final concentration) and used as controls. All five bottles were inoculated with a sterile solution of 7.9 mM 2-(ρ-iodophenyl)-3-(ρ-nitrophenyl)-5phenyl tetrazolium chloride salt (INT) to give a final concentration of 0.8 mM. The solution was freshly prepared for each experiment using Milli-Q water. The INT samples were incubated in the same temperature controlled incubators as the dissolved oxygen bottles for 0.5 to 1.4 h and then the three

237 replicates were fixed by adding formaldehyde, as described above for the two controls.
238 Samples were sequentially filtered through 0.8 μm and onto 0.2 μm pore size polycarbonate
239 filters, air-dried, and stored frozen in 1.5 mL cryovials at –20 °C until further processing. The
240 INT reduced in each fraction (i.e. >0.8 μm and 0.2-0.8 μm) was determined from the
241 absorbance at 485 nm of the reduced INT (formazan), extracted with propanol and measured
242 in quartz cuvettes using a Beckman model DU640 spectrophotometer following Martínez-
243 García et al. (2009). The mean of the INT reduction in the two controls was subtracted from
244 the INT reduction measured in the three incubated replicates, thus correcting for any
245 interference of the absorbance of the water due to turbidity and reduction of INT caused by
246 non-metabolic factors (i.e. organic matter content) (average 52 ± 1 % of absorbance in the
247 incubated samples). The rate measured in the large size-fraction ($INT_{>0.8}$) will result mainly
248 from INT reduction by eukaryotes and particle attached bacteria. By contrast, the main
249 respiring organisms in the small size-fraction ($INT_{0.2-0.8}$) would be heterotrophic bacteria. The
250 total microplankton community respiration (INT_T) is calculated as the sum of the INT
251 reduction in the two size fractions ($INT_{0.2-0.8}$ and $INT_{>0.8}$).

252 Time-course experiments were carried out on seawater collected from 5 m on the 11th
253 November 2014, 4th April 2015 and 14th July 2015 in order to determine the optimal
254 incubation time for INT reduction. The maximum incubation time before the INT became
255 toxic for the plankton (seen as a decrease in the INT reduction rate due to the negative effect
256 on cell activity of the intracellular deposition of formazan) was found to be 2, 1 and 1 h, in
257 November, April and July respectively. Hence, all our incubations were undertaken for
258 shorter times than these (<1.4 h <0.8 h, <0.5 h, respectively). INT reduction was converted
259 into dissolved oxygen consumption using the equation: moles $O_2 = 2.82*molesINT^{0.806}$
260 derived from the comparison of CR_{O2} and INT_T rates from this study ($R^2 = 0.43$, $p < 0.0001$, n
261 = 97, Fig. 2). Heterotrophic bacterial respiration in moles of C was calculated from the

$INT_{0.2\text{-}0.8}$ reduction rates converted into units of dissolved oxygen consumption and applying a respiratory quotient of 1.

2.7 Heterotrophic bacterial production and bacterial growth efficiency

Water samples for heterotrophic bacterial production (BP) were collected from the same 6 Niskin bottles as the samples for determination of microplankton community and bacterial respiration detailed above, into 125 mL acid washed polycarbonate bottles. Aliquots of 10 µL ^{14}C leucine working solution (0.04 MBq mL^{-1}) were pipetted into 2 mL sterile centrifuge tubes with 1.6 mL of sample water and mixed. For each depth, duplicate samples were incubated for 0, 1, 2 and 3 h in the dark at temperatures representative of the depth of collection. Samples were fixed with 80 µL of 20 % paraformaldehyde (final concentration of 1 %). The duplicate samples were filtered onto 0.2 µm polycarbonate filters pre-soaked in 1 mM non-labelled leucine on top of a 25 mm GF/F filter as a backing filter. Each 0.2 µm polycarbonate filter was placed into a scintillation vial, dried overnight at room temperature in a fumehood and mixed with 4 mL of Optiphase Hi-Safe II scintillation fluid. Radioactivity in the samples was measured using a Beckman Coulter LS6500 liquid scintillation counter. Bacterial population growth (cells m^{-3} d^{-1}) was calculated from ^{14}C leucine incorporation using a theoretical approach assuming no isotope dilution (Kirchman 2001).

Cell-specific bacterial production and respiration were calculated by normalizing BP and $INT_{0.2\text{-}0.8}$ to BA, respectively. Bacterial carbon demand (BCD) was calculated as: BP +$INT_{0.2\text{-}0.8}$ and bacterial growth efficiency (BGE) as: BP/BCD.

2.8 Data analysis

Depth-integrated Chl-*a*, ^{14}C-PP, CR_{O2}, $INT_{T,}$ $INT_{>0.8}$, $INT_{0.2\text{-}0.8}$ and BP rates were calculated by trapezoidal integration of the volumetric rates measured in the UML. The standard errors (± SE) of the integrated rates were calculated following the propagation procedure for independent measurements described by Miller and Miller (1988). The depth-integrated contribution of the 0.2-0.8 μm fraction to total microplankton community respiration ($\%INT_{0.2\text{-}0.8}$) was calculated as the depth-integrated $INT_{0.2\text{-}0.8}$ divided by the depth-integrated INT_T and multiplied by 100.

Statistical analyses were performed with SPSS statistical software on log-transformed data where necessary. A two-way ANOVA was used to determine the effects of month and station and any interacting effects between these two factors on BA, CR_{O2}, INT_T, $INT_{0.2\text{-}0.8}$, $\%INT_{0.2\text{-}0.8}$ and BP. Paired t-tests were performed to verify significant differences between $CR_{O2,}$ $INT_{0.2\text{-}0.8}$, $\%INT_{0.2\text{-}0.8}$, BP, cell-specific $INT_{0.2\text{-}0.8}$ and cell-specific BP in the UML and BML. In order to be able to compare the two layers, the UML depth-integrated rate was divided by the depth of integration to derive the rate per cubic metre (weighted metabolic rate). Spearman non-parametric correlation tests were used to determine the relationship between volumetric BA, CR_{O2}, INT_T, $INT_{0.2\text{-}0.8}$, BP, BCD and BGE and between each of these and environmental parameters (temperature, nitrate+nitrite concentration, phosphate concentration, silicate concentration, Chl-*a* concentration and *p*DOC). Non-parametric multivariate techniques were used with the PRIMER v 6.1 statistical package to discern station grouping based on the microplankton autotrophic metabolic rates (^{14}C-PP, *p*DOC), microplankton heterotrophic metabolic rates (CR_{O2}, $INT_{>0.8}$, $INT_{0.2\text{-}0.8}$, $\%INT_{0.2\text{-}0.8,}$ BP and BGE) and to relate these to the environmental data (temperature, nitrate+nitrite, phosphate, silicate concentration, Chl-*a*, bacterial abundance, DOC and DON concentration). A Bray-Curtis similarity matrix was constructed from the standardized data of the microplankton metabolic parameters and Euclidean distances were calculated on the normalized

environmental data. Sampling days were classified using distance based redundancy analysis (dbRDA) (Legendre & Anderson, 1999). A distance-based linear model (distLM) was used to analyse the relationships between microplankton metabolism and environmental parameters.

RESULTS

3.1 Hydrographic conditions

A full description of the hydrographic and nutrient conditions present in the Celtic Sea during the sampling period (November 2014, April 2015 and July 2015) is reported in Poulton et al., (this issue), Humphreys et al., (this issue) and Wihsgott et al., (this issue) and a brief overview given in Table 1.

The seasonal variability in hydrography followed the typical progression for temperate shelf seas. November was characterized by thermal homogeneity of the upper 55 m of the water column with weak stratification occurring in deeper waters. These conditions are typical for a late summer-early autumn situation when the complete disruption of the summer thermocline has not yet occurred. During November, upper mixing layer temperatures were 12 to 14 ˚C and salinity was slightly lower at the surface than in deeper waters (difference <0.1). There was a weak thermocline at the beginning of April at 65 m which was strengthened by the end of April (Table 1, Wihsgott et al., this issue). Temperatures in April (ranging from 9.8 – 11.2 ˚C) were lower than in November (11.2 – 13.7 ˚C) with warmer waters at the surface and colder waters at depth. Thermal stratification prevailed during July with sea surface temperatures >15.5 ˚C in the UML, and <11.5 ˚C in the BML. In November the UML extended to 92 m at CCS and to 119 m at CS2. In April there was a shallowing of the UML from 65 m on 4th April to 45 m on 25th April at CCS. However, the UML remained at 65 to 70 m at CS2 during April. In July, the UML occurred between 50 and 56 m at both stations.

3.2 Seasonal patterns of chlorophyll-*a* and bacterial abundance

The vertical distribution of Chl-*a* and BA differed between the two stations. At CCS, surface Chl-*a* concentration was higher in November (1.3-1.7 mg Chl-*a* m^{-3}) than in July (0.3 mg Chl-*a* m^{-3}) and the highest concentrations (~3-6 mg Chl-*a* m^{-3}) were found in April with the development of the phytoplankton bloom (Poulton et al. this issue; Hickman et al. this issue). In general at CCS, the vertical profile of Chl-*a* was characterised by a homogenous vertical distribution in November, and development of a subsurface peak above the nitracline (~25 m in April and 45 m in July) and lower concentrations (<2 mg Chl-*a* m^{-3}) at depth in April and July. At CS2, Chl-*a* concentrations were <1 mg Chl-*a* m^{-3} in November and July with a well-mixed vertical distribution and were around 1.5 mg Chl-*a* m^{-3} in April with a subsurface peak above the base of the UML coincident with the base of the nitrate+nitrite gradient (Humphreys et al., this issue).

The vertical distribution of bacterial abundance was similar to the Chl-*a* distribution at both stations (Fig. 3A, 3G). In general at CCS, BA varied little with depth in November and April in the UML (0.6-0.7 and 1.4 $x10^6$ cells mL^{-1}, respectively), whereas July was characterised by a BA subsurface maximum (1.3-1.7 $x10^6$ cells mL^{-1}) at the base of the UML. Bacterial abundance was similar at CCS and CS2 in November and April, but was higher at CS2 than at CCS in July with concentrations in surface waters of >1.4 $x10^6$ cells mL^{-1} and a progressive decrease to 0.4 $x10^6$ cells mL^{-1} at the base of the UML.

Depth-integrated bacterial abundance had the highest and lowest values in April (7.2 $x10^{13}$ and 3.3 $x10^{13}$ cells m^{-2}) at CCS, and there was no seasonal variability at CS2 (Fig. 4A).

3.3. Seasonal patterns of microplankton community respiration and bacterial activity

Daily (CR_{O2}) was positively correlated (r = 0.62, p <0.0001, n = 97, Fig. 2) with hourly (INT_T) rates of microplankton community respiration. However, there were differences in the magnitude of the rates derived from the two methods, with INT_T rates greater than CR_{O2} in November and April but lower in July (Fig. 3B-C). These dissimilarities could be due to several reasons. The two methods measure over different time scales (<1.4 - 24 h), so that any reduction in grazing pressure due to enclosure in relatively small bottles, could lead to a greater increase in bacterial abundance over the longer incubation times required for CR_{O2} than those for INT_T. The different time scales might also lead to differences in community structure and therefore respiration. The relationship between paired community respiration measurements (CR_{O2} and INT_T) differed between data collected in November and that collected in April and July (Clarke test, p <0.001; Clarke 1980). There was no statistical difference between the slope of the paired measurements in April and July (Clarke test, p = 0.23) (Fig. 2). The dissimilarity between the slopes of November CR_{O2}:INT_T data and April and July CR_{O2}:INT_T data may be caused by the high variability in the low rates measured in November, the small range of CR_{O2} and INT_T rates measured in November, or the change in plankton community composition with different plankton having different abilities to take up INT. Due to the low number of data collected in each month, a single CR_{O2}:INT_T conversion model was derived from data collected in all three months (see section 2.6) (Fig. 2).

Differences in the monthly average vertical distribution of CR_{O2} corresponded to monthly changes in the vertical distribution of Chl-*a* concentrations (Fig. 3B, 3H). At CCS, higher CR_{O2} rates (3.6 and 1.8 µmol O_2 L^{-1} d^{-1}, in April and July respectively) were measured coincident with the Chl-*a* maxima which in April was at ~15 m and in July at ~42 m, while CR_{O2} and Chl-*a* were homogeneously distributed in November. At CS2, subsurface peaks in CR_{O2} occurred in November and April whereas in July CR_{O2} gradually decreased from the surface to the base of the UML. The subsurface maxima in CR_{O2} and INT_T in April at CCS

383 and in July at CS2 were due to an increase in the respiration of the plankton fraction >0.8 µm
384 (Fig. 3D & 3J). Monthly average depth-integrated rates of CR_{O2} varied seasonally by 1.2 to
385 2.8-fold, with the highest rates in April (164 ± 5 mmol O_2 m^{-2} d^{-1}) and the lowest in
386 November (27 ± 4 mmol O_2 m^{-2} d^{-1}) at CCS (Fig. 4B). The seasonal range was smaller at CS2
387 where the highest depth-integrated rates of CR_{O2} were measured in April (78 ± 6mmol O_2 m^{-2}
388 d^{-1}) and the lowest in November (45 ± 9 mmol O_2 m^{-2} d^{-1}).

389 Monthly average rates of heterotrophic bacterial respiration did not show any vertical trend at
390 either of the stations (Fig. 3E & 3K). Depth-integrated $INT_{0.2-0.8}$ was highest and most
391 variable in April (12 - 32 and 14 - 21 mmol O_2 m^{-2} d^{-1} at CCS and CS2, respectively) and
392 lowest in July (7 - 10 and 11 mmol O_2 m^{-2} d^{-1} at CCS and CS2, respectively) (Fig. 4C). Cell-
393 specific heterotrophic bacterial respiration was highest in the middle of April (0.51 ± 0.05
394 and 0.89 ± 0.11 fmol O_2 $cell^{-1}$ d^{-1} at CCS and CS2, respectively), and lowest in July (0.14 ±
395 0.02 and 0.23 ± 0.03 fmol O_2 $cell^{-1}$ d^{-1} at CCS and CS2, respectively) (Table 2), due to a
396 combination of high bacterial numbers and low bacterial respiration. There were no
397 significant differences in cell-specific heterotrophic bacterial respiration between months,
398 stations and the interaction of month and stations (Two-way ANOVA, p >0.05).

399 The monthly average proportion of depth-integrated microplankton community respiration
400 attributable to bacteria (%$INT_{0.2-0.8}$) at CCS was higher (37 ± 4%) in November, than in April
401 (21 ± 5 %) or July (19 ± 3 %) (Fig. 4D). At CS2, the highest %$INT_{0.2-0.8}$ occurred in April (42
402 ± 6 %) and the lowest in July (27 ± 4 %).

403 Monthly average bacterial production rates were in general higher in sub-surface waters (5 –
404 20 m) and decreased with depth (Fig. 3F & 3L). The seasonal vertical pattern in BP differed
405 from that of $INT_{0.2-0.8}$ with the highest BP rates occurring in July (0.4 and 0.48 µmol C L^{-1} d^{-1}
406 at CCS and CS2, respectively) and the lowest in November (<0.1 and <0.08 µmol C L^{-1} d^{-1} at

CCS and CS2, respectively). Upper mixing layer depth-integrated BP showed no significant differences between stations and the interaction of stations and months (Two-way ANOVA, p >0.05), but significant differences existed between months (p = 0.01) with the highest rates in July and the lowest in November (Fig. 4E). Depth-integrated BP was 2-fold higher at CCS than at CS2 in April, but there was no difference in BP between stations in November or July. Cell-specific BP was significantly different between months (Two-way ANOVA, p = 0.013), but not between stations or the interaction of stations and months (Two-way ANOVA, p >0.05). Monthly average cell-specific BP was higher in July (0.32 ± 0.01 pmol C cell^{-1} d^{-1}) than in November (0.15 ± 0.02 pmol C cell^{-1} d^{-1}) or April (0.22 ± 0.02 pmol C cell^{-1} d^{-1}) (Table 2).

There was no difference in UML depth-integrated bacterial carbon demand (BCD) (Table 2) between stations and months (Two-way ANOVA, p >0.05). In general, the volumetric BCD was always lower than the amount of dissolved organic carbon produced by phytoplankton as a result of photosynthesis (*p*DOC) (Fig. 5).

Depth-integrated bacterial growth efficiency (BGE) ranged from 18 % to 71 % (Table 2) with significantly higher (Two-way ANOVA, p <0.05) BGEs in July (average ± SE, 61 ± 5 %) than in November (27 ± 3 %) and April (36 ± 6 %). No significant differences in BGE were found between stations and the interaction of stations and months (Two-way ANOVA, p >0.05).

3.4 Plankton metabolism and relationships with environmental and biological data

The correlation matrix of the volumetric variables (Table 3) shows how microplankton community respiration and bacterial production and respiration were related differently to the physicochemical and biological characteristics of the water column. Taking all volumetric

data together, CR_{O2} was positively correlated to total Chl-*a* concentration, *p*DOC, bacterial abundance and bacterial production and negatively correlated to nitrate+nitrite and phosphate concentrations. $INT_{0.2\text{-}0.8}$ was positively correlated to Chl-*a*, silicate concentrations and bacterial abundance and negatively correlated to temperature. Bacterial production was positively correlated to Chl-*a*, ammonium concentration, bacterial abundance and microplankton community respiration and negatively correlated to nitrate+nitrite, silicate and phosphate concentrations. The negative correlations observed between CR_{O2}, BP and nitrate+nitrite are likely caused by the covariation between depth and nitrate+nitrite, as deep waters had higher nitrate+nitrite concentration and lower respiration rates due to lower Chl-*a* and bacterial abundance. Phytoplankton *p*DOC, which is an indicator of the amount of substrate (DOC) available to the bacteria, was positively correlated with microplankton community respiration, bacterial production and bacterial abundance. The analysis of the correlation between UML depth-integrated CR_{O2}, $INT_{0.2\text{-}0.8,}$ BP and BGE with the UML depth-integrated dissolved organic carbon and nitrogen (DOC and DON) concentrations showed different trends. CR_{O2}, BP and BGE were negatively correlated to DOC (r = -0.79, p <0.01, n =10 for CR_{O2}; r = -0.85, p <0.001, n =11 for BP; and r = -0.88, p <0.001, n =10 for BGE) while $\%INT_{0.2\text{-}0.8}$ was positively correlated (r = 0.88, p <0.001, n = 10). DON was positively correlated with $\%INT_{0.2\text{-}0.8}$ (r = 0.68, p = 0.03, n = 10) and negatively correlated with BP (r = -0.7, p = 0.16, n = 11) and BGE (r = -0.76, p = 0.01, n = 10) (Fig. 6).

Ordination analysis of the environmental and metabolic rates provides a better understanding of the relationships between the environmental data and microplankton metabolism during the different months. The analysis was performed separately on the weighted UML depth-integrated microplankton autotrophic (^{14}C-PP, *p*DOC) and heterotrophic (CR_{O2}, $INT_{>0.8,}$ $INT_{0.2\text{-}0.8}$, $\%INT_{0.2\text{-}0.8}$, BP and BGE) metabolic rates. Distance based redundancy models were used to study the relationship between the environmental variables (weighted UML depth-

integrated temperature, nitrate+nitrite, phosphate, silicate, ammonium, DOC and DON concentration, Chl-*a* and bacterial abundance). Results from this analysis indicated that 56 % of the variability in microplankton autotrophic responses and 85 % of the variability in microplankton heterotrophic responses could be explained by two axes. The environmental variables that best explained the microplankton autotrophic metabolic rates were a combination of temperature, DON concentration, bacterial abundance and nitrate+nitrite concentration (Fig. 7A). By contrast, Chl-*a*, nitrate+nitrite, silicate, ammonium, DON concentration and bacterial abundance better described the microplankton heterotrophic metabolic rates (Fig. 7B) which accounted for 100 % of the fitted model variation. The ordination analysis of the autotrophic metabolic rates separated all April data at CCS from the other sampling days. Within the heterotrophic metabolic rates, three groups could be observed: Group I consists of the majority of the April data (11^{th}, 15^{th}, 20^{th} and 25^{th} April) at CCS, Group II is formed by all July data (CCS and CS2), and Group III consists of November data together with the April data at CS2 and data collected on the 4^{th} April at CCS.

3.5 Carbon cycling in the upper versus bottom mixing layers

Daily rates of microplankton community respiration, heterotrophic bacterial respiration and production in the UML were compared with the corresponding rates in the BML in the different months by paired-*t* test. Due to the low number of measurements made per month at CS2 ($\leq$2), statistical tests were only performed on data from CCS.

Within month variability in CR_{O2}, $INT_{0.2\text{-}0.8}$ and BP was high, especially in April when the phytoplankton bloom developed (Fig. 8). At CCS, CR_{O2} in the UML was significantly higher than CR_{O2} in the BML (p <0.032) in all months (Fig. 8A).

479 $INT_{0.2\text{-}0.8}$ was not significantly different above and below the thermocline (Fig. 8C). In
480 addition, there was no significant difference between UML and BML cell-specific bacterial
481 respiration in any of the months (p >0.05), which indicates that lower bacterial numbers in
482 the BML sustained lower bacterial respiration (Fig. 8I). There was also no significant
483 difference between the percentage of microplankton community respiration attributable to
484 bacteria in the UML and BML (p >0.05) (Fig. 8E).

485 BP in the UML was significantly different to that in the BML in November, April and July (p
486 <0.04). BP rates were between 3 and 7-fold higher in the UML than in the BML with the
487 greatest difference occurring in July (Fig. 8G). In contrast, cell-specific bacterial production
488 was only significantly different between the two depth layers in April and July (p = 0.001,
489 both cases) with 2.5- and 5-fold higher cell-specific bacterial production in the UML than in
490 the BML in April and July, respectively (Fig. 8K).

491

492 **DISCUSSION**

493 **4.1 Central Celtic Sea versus Shelf Edge**

494 Recent studies in the Celtic Sea have demonstrated differences in the physicochemical
495 properties between the central Celtic Sea and the shelf edge (Sharples 2001, 2009). The shelf
496 edge station (CS2) is characterized by higher turbulent mixing which supports a
497 phytoplankton community dominated by larger cells (> 20 µm), whereas phytoplankton in the
498 central Celtic Sea are dominated by smaller cells (2 – 20 µm) (Sharples 2009, Hickman et al.,
499 2012, this issue). In the present study, water column stratification differed between the CCS
500 station and the shelf edge CS2 station. In April and July, there was a well-defined UML and
501 BML separated by a thin thermocline at CCS while at CS2 the thermal gradient was less
502 distinct and occurred over a broader depth interval (data not shown). There were, therefore,

differences in the depth of the upper mixing layers between the two stations, in the depth of the Chl-*a* subsurface maximum (deeper in the CCS than at CS2), which drove changes in the vertical distribution of microplankton community respiration and bacterial production. However, these differences in hydrodynamic conditions were not reflected in differences in UML depth-integrated CR_{O2}, $INT_{0.2-0.8}$ or BP, except in April. In April, the higher increase in CR_{O2} at CCS than at CS2 may be related to the different Chl-*a* concentrations measured at the two stations (94 ± 15 and 48 ± 11 mg Chl-*a* m^{-2}, respectively). At CCS, thermal stratification developed as a consequence of the warming of surface waters contributing to ideal conditions (increase in stability, high nutrient concentrations and solar energy) for phytoplankton growth leading to the spring bloom (Wihsgott et al., this issue). In contrast, at CS2, the hydrodynamic conditions did not promote phytoplankton growth and therefore there was relatively little increase in Chl-*a* concentration (data not shown), microplankton community respiration or bacterial production. The higher BP rates at CCS than at CS2 in April contrast with a previous study in the Celtic Sea in April 1987 where the BP was 2-fold higher in the mixed water at the shelf edge than in the stratified waters of the continental shelf (Martin-Jézéquel and Videau 1992).

The lack of difference in the depth integrated rates between stations may be caused by the difference in the depth of integration, which was 30 m and 13 m deeper at CS2 than at CCS in November and April, respectively. In fact, the ordination analysis that compares the weighted microplankton metabolic rates at the different stations indicated that the plankton metabolism in April at CS2 was similar to that in November at CCS. The strong internal waves and internal tidal mixing (Pingree et al. 1983, Sharples et al. 2009), establish differences not only in the phytoplankton distribution (Sharples et al. 2009) but also in the microplankton metabolism in the Celtic Sea.

4.2 Carbon metabolism of microplankton communities

Rates of CR_{O2} measured during this seasonal study lie within the range of previous measurements made in the Celtic Sea (Robinson et al. 2009) and North Atlantic shelf seas (Blight et al. 1995, Serret et al. 1999, Arbones et al. 2008) (Supplementary Table 1). Our range of $INT_{0.2\text{-}0.8}$ (0.03 – 0.85 µmol O_2 L^{-1} d^{-1}) corresponds with bacterial respiration rates measured in a seasonal study in the open Mediterranean Sea (Lemée et al. 2002) and lies at the lower end of the rates measured in the North Sea (Reinthaler and Herndl, 2005) and in a seasonal study in the northwest coastal region of the Mediterranean Sea (Alonso-Sáez et al. 2008). Our UML depth-integrated BP is between 8 and 50-fold greater than the euphotic depth-integrated BP measured in the Celtic Sea by Joint and Pomroy (1987) yet is 3-fold lower than BP measured by Davidson et al. (2013) in July 2008 in the area around CCS (49.8 ˚N, 7.8 ˚W). The difference between our measurements and those of Joint and Pomroy (1987) is likely caused by the different methodologies (thymidine uptake versus leucine uptake) used. Bacterial production derived from thymidine and leucine assimilation can be different because the leucine to thymidine incorporation ratio is not constant (Li et al. 1993, Pomroy and Joint 1999). In fact, a leucine and thymidine incorporation study performed in the Oregon coast reported 10-fold differences in the leucine and thymidine incorporation for bacterial cells (Longnecker et al. 2006). This large difference between rates due to different methods complicates direct comparison between our study and that of Joint and Pomroy (1987). During July the difference between the euphotic layer (considered as the layer between the surface and the depth at which incident irradiance is 1 % of surface irradiance) and the UML in our study ranged between 3 to 4 meters, so the difference in the depth of integration (euphotic depth versus the upper mixing layer depth) is unlikely to be the cause of the discrepancy between Davidson et al. (2013) and our data. In addition, the leucine methodology and the isotope dilution factor were similar for the two studies. Therefore, the

553 differences in the bacterial production rates between Davidson et al. (2013) and our data may
554 be associated to inter-annual variability.

555 Our depth-integrated BGE ranged from 18 to 71 %, in line with the range of BGEs compiled
556 by del Giorgio and Cole (1998) and the 3 to 71 % range reported by Sintes et al. (2010) in the
557 North Sea, but higher than the 5 to 28 % range measured previously by Reinthaler and Herndl
558 (2005) in the North Sea. The differences between the former estimates and those in the
559 present study may be due to differing methodologies. Reinthaler and Herndl (2005) and
560 Sintes et al. (2010) estimated bacterial respiration from dissolved oxygen consumption in pre-
561 filtered samples incubated for 24 h, while our estimates are based on INT reduction in
562 incubations lasting <1.4 h. Incubating pre-filtered water samples can lead to overestimates of
563 bacterial respiration (Aranguren-Gassis et al. 2012). Therefore, BGE in the former studies
564 (Lemée et al. 2002, Reinthaler and Herndl 2005, Sintes et al. 2010) may have been
565 underestimated. However, our $INT_{0.2\text{-}0.8}$ rates, determined from samples filtered onto 0.2 µm
566 filters, could also be underestimated, due to the loss of bacterial cells less than 0.2 µm in
567 diameter. Bacterial abundance in the 0.2 µm filtered water in July corresponded on average
568 (n = 7) to 30 ± 2 % of the BA in the unfiltered sample (data not shown). The percentage of
569 bacteria passing through the 0.2 µm filter in this study is slightly higher than the 2 to 26 %
570 values reported by Gasol and Morán (1999). Thus, assuming a constant cell-specific
571 respiration rate of all 0.2 - 0.8 µm bacteria, the bacterial respiration derived from $INT_{0.2\text{-}0.8}$
572 could be underestimated by ~30 %. Recalculating BCD and BGE, using $INT_{0.2\text{-}0.8}$ increased
573 by 30 %, results in an increase on the monthly average BCD of the two stations of 24, 21 and
574 12 % in November, April and July and a decrease in the monthly average BGE of 19, 17 and
575 10 %, respectively. Overall, the rates of microplankton and bacterioplankton metabolism
576 measured here are comparable to previous rates measured in North Atlantic shelf seas.

577

578 **4.3 Seasonal variability**

579 The seasonal changes in environmental conditions occurring in the Celtic Sea were reflected
580 in pronounced seasonality of CR_{O2} in the UML, with a minimum in November and a
581 maximum in April. The increase in Chl-*a* concentration (an indicator of increased
582 phytoplankton abundance) in April was associated with an increase in the respiration of the
583 >0.8 µm size fraction of the plankton community, and thus CR_{O2}. In general, heterotrophic
584 bacterial respiration only contributed 38, 24 and 21 % of the microplankton community
585 respiration in November, April and July, respectively. Despite the increase in the production
586 of organic matter by phytoplankton in April (Fig. 5, Poulton et al. this issue, Mayers et al. this
587 issue), the $INT_{0.2-0.8}$ did not show a corresponding increase. This constancy in rates of
588 heterotrophic bacterial respiration, despite a 3.8 and 1.4-fold greater average phytoplankton
589 DOC production in April than in November and July, respectively, contrasts with previous
590 studies where bacterial respiration was enhanced by organic matter synthesized by
591 phytoplankton during bloom periods (Blight et al. 1995, Alonso-Sáez et al. 2008). This may
592 suggest that heterotrophic bacterial respiration in our study was not controlled by the
593 availability of organic matter but by limiting concentrations of inorganic nitrogen or
594 phosphorus (Rivkin and Anderson 1997, Kirchman 2000). However, since there was an
595 increase in bacterial abundance and bacterial production, it seems that bacterial activity was
596 not limited by inorganic nutrients.

597 BP showed a seasonal trend, with the highest rates occurring at the end of April and in July
598 and the lowest rates occurring in November. Therefore, bacteria appear to use the newly
599 produced dissolved organic matter to produce more bacterial biomass while maintaining low
600 respiration levels in April and July. Another explanation for the lack of a seasonal trend in
601 bacterial respiration might be related to a seasonal change in bacterial community
602 composition (Gilbert et al. 2009, 2012, Tarran et al. this issue) between bacterial groups with

603 different specific respiration rates (del Giorgio and Gasol 2008) and differing ability to take
604 up INT. The INT reduction technique has been used for microplankton organisms (Martínez-
605 García et al. 2009), but a comprehensive suite of culture experiments confirming that all
606 representative groups of bacterioplankton can equally take up and reduce INT has not yet
607 taken place. Such experiments are required to confirm that $INT_{0.2\text{-}0.8}$ does not underestimate
608 bacterial respiration when particular bacterioplankton groups, which are less able to take up
609 INT, are dominant.

610 Seasonal variability in CR_{O2} and BP has been previously observed in coastal systems (Blight
611 et al. 1995, Griffith and Pomroy 1995, Serret et al. 1999, Alonso-Sáez et al. 2008, Arbones et
612 al. 2008, Céa et al. 2014). Highest CR_{O2} rates in the present study coincided with maximum
613 values of primary production determined by radiolabelled bicarbonate uptake (^{14}C-PP) (Fig.
614 9), and these two indicators of plankton metabolism were positively correlated (r = 0.47, p
615 <0.0001, n = 72). These observations are in agreement with previous seasonal studies where
616 the highest respiration rates were measured during the time of highest phytoplankton
617 abundance (Blight et al. 1995, Serret et al. 1999, Maixandeau et al. 2005, Arbones et al.
618 2008). However, minimum CR_{O2} values were measured in November in the Celtic Sea,
619 despite the Chl-*a* concentrations being higher in November (average ± SE, 1.29 ± 0.05 µg
620 Chl-*a* L^{-1}) than in July (0.66 ± 0.11 µg Chl-*a* L^{-1}). Zooplankton abundance may influence the
621 seasonal differences in plankton community respiration (Joint et al. 2001) as intermediate
622 CR_{O2} values were measured in July when Chl-*a* was lowest, but mesozooplankton (>200 µm)
623 and nauplii abundance was high (Tarran et al. this issue, Giering et al. this issue). The low
624 Chl-*a* values combined with the low $\%INT_{0.2\text{-}0.8}$ found in July support our suggestion that
625 zooplankton had a higher contribution to CR_{O2} in July, leading to high CR_{O2} rates.
626 Interestingly, the relationship between ^{14}C-PP and CR_{O2} showed distinctive patterns in April
627 and July (Fig. 9). The linear regression slope between ^{14}C-PP and CR_{O2} was higher in July

(0.78 ± 0.12), and statistically indistinguishable from unity (Clarke test, t = 1.4, df = 35, p = 0.17), while in April the slope was lower (0.15 ± 0.02) and statistically different from unity (Clarke test, t = 16, df = 70, p <0.0001). The difference in the ^{14}C-PP:CR_{O2} ratio indicates that the system was in balance during July, and acted as a sink of CO_2 and source of organic matter in April, with this surplus of organic matter consumed by bacteria and/or zooplankton, or horizontally and vertically transported.

The seasonal variability in BCD and BGE was driven by changes in BP, which increased 2-fold from November to July, and in $INT_{0.2-0.8}$ which decreased 2-fold from November and April to July. The published seasonal studies which measured BGEs in temperate coastal regions all showed seasonal variability (Lemée et al 2002, Reinthaler and Herndl 2005, Vázquez-Domínguez et al. 2007, Alonso-Sáez et al. 2008, Sintes et al. 2010, Céa et al. 2014), but there is no single environmental variable which consistently drives the variability in BGE. On the one hand, several researchers found that the seasonal variability in BGE was driven by changes in bacterial respiration (Sherry et al. 1999, Lemée et al. 2002, Vázquez-Domínguez et al. 2007). Whereas, other researchers concluded that bacterial production influenced the changes in BGEs (del Giorgio and Cole 2000, Reinthaler and Herndl 2005,). The present study shows that the variability in both BP and $INT_{0.2-0.8}$ determined the variability of BGE and that the two variables have different influences depending on the month (BP was the dominant inflence in November and April, while both BP and $INT_{0.2-0.8}$ drove the changes in July). However, this does not reveal which environmental conditions drive the changes in BP and $INT_{0.2-0.8}$, and therefore BGE. Production of dissolved organic carbon by phytoplankton did not control the changes in BGE and the relationships between environmental conditions (i.e. temperature and nutrient concentrations) and BGE were different in November, April and July. Therefore, a combination of several factors which may act simultaneously, and may be different during different months, influenced BGE. Ordination analysis showed that

653 different environmental parameters were influencing the autotrophic and the heterotrophic
654 metabolic rates differently during the three months. In April, microplankton heterotrophic
655 metabolism at CCS was related to a decrease in nitrate+nitrite and increase in Chl-*a*
656 concentration, while in July microplankton heterotrophic metabolism was related to an
657 increase in ammonium and bacterial abundance.

658

659 **4.4 Consumption of phytoplankton produced dissolved organic carbon by bacteria**

660 Previous studies show that during productive periods bacterial carbon requirements are
661 sustained by concurrent phytoplankton DOC production, while external DOC inputs are
662 required to fulfil the BCD during unproductive times (La Ferla et al. 2006). In contrast to
663 these results, in the present study DOC production derived from phytoplankton
664 photosynthesis was always higher than BCD, irrespective of the time of year (Fig. 5). Even if
665 we consider that our BCD calculations are underestimated (see above) and we recalculate the
666 BCD with an increase of 30 % in heterotrophic bacterial respiration, the *p*DOC was still
667 greater than the recalculated BCD for all concurrent data. The *p*DOC:BCD >1 suggests that
668 bacterial metabolism was not limited by resources, as there was always sufficient DOC
669 produced by phytoplankton to satisfy the bacterial requirements. Therefore phytoplankton
670 and bacterial metabolism were coupled, considering "coupling" to be the capacity of
671 phytoplankton to produce enough dissolved primary production (*d*PP) to meet the BCD
672 (Morán et al. 2002). However, the magnitude of bacterial carbon demand was not dependent
673 on the amount of organic carbon produced by phytoplankton, as shown by the lack of
674 relationship between *p*DOC and BCD within each month (Fig. 5). Morán et al. (2002)
675 investigated the relationship between BCD and production of dissolved organic carbon in
676 different ecosystems (Antarctic offshore, Antarctic coastal, NE Atlantic NW Mediterranean),

677 calculating BCD from bacterial production data collected in situ and assuming a constant
678 BGE of 7.1, 15 and 30 %. They concluded that the "*BCD would on average always exceed*
679 *dissolved primary production in the NE Atlantic, unless unrealistically high BGEs were*
680 *used*". Contrary to their conclusion, our BCD values were always lower than the *p*DOC
681 (considered as dissolved primary production) at a broad range of BGE values (18 - 71 %)
682 suggesting a good coupling between bacteria and phytoplankton.

683

684 **4.5 Upper mixing layer versus bottom mixing layer**

685 Light, nutrients, phytoplankton biomass, and community structure may have a major control
686 on microplankton metabolism in the UML and BML. In general, the BML was characterized
687 by low light intensities (<0.1 % of the I_0), lower temperatures and higher nutrient
688 concentrations. The temperature difference between the two layers was <1 ˚C in November
689 and April and ~ 2.5 ˚C in July. Bacterial metabolism is positively related to temperature
690 (Kirchman et al. 2005, Vázquez-Domínguez et al. 2007, Kritzberg et al. 2010). However, we
691 found similar cell-specific bacterial respiration rates in the UML and BML, no relationship
692 between temperature and BP, and furthermore the ordination analysis did not select
693 temperature as a major variable separating microbial heterotrophic metabolic rates (Fig. 7B).
694 Similar concentrations of DOC and DON were measured in the UML and BML (Davis et al.
695 this issue), except in July when DOC and DON were lower in the BML than in the UML.
696 Therefore, the composition of the organic matter (C:N ratio) was not a major influence on the
697 differences observed in microplankton metabolism.

698 CR_{O2} and BP were higher in the UML than in the BML (4-fold and 7-fold, respectively)
699 presumably as a result of the larger amount of phytoplankton and bacteria in the UML than
700 the BML. However, $INT_{0.2\text{-}0.8}$ and cell-specific bacterial respiration were similar in both

layers. It seems that the interactions between phytoplankton and bacteria were favouring bacterial production in the UML, in contrast to the low bacterial production in the BML. Release of DOC from phytoplankton is one of several interactions existing between phytoplankton and bacteria (Cole 1982, Amin et al. 2012). The organic carbon released by phytoplankton has been shown to be used as a substrate for bacteria (Cole 1982, Baines and Pace 1991, Morán et al. 2002), enhancing bacterial respiration and bacterial production. In our study, the DOC produced by phytoplankton only stimulated the bacterial production, as there was no correlation between the $INT_{0.2-0.8}$ and *p*DOC. The use of organic compounds only for growth rather than respiration could be considered a survival response. For example, in April, when the inorganic nutrients start to decline due to phytoplankton uptake, and the direct competitors for nutrients (phytoplankton) are increasing in number, bacteria in the UML could have used the *p*DOC to increase their production at similar respiration rates.

Overall, our results contrast with a previous study in the North Sea, where they reported a separation in the water column of consumption of dissolved inorganic carbon (DIC; primary production), which occurred in the surface layers, from DIC production (respiration) which occurred in the bottom mixed waters (Thomas et al. 2004). In this former study, the enhancement of respiration processes below the mixing layer during a stratified period increased the transport of CO_2 from the shelf sea to the open ocean (Thomas et al. 2004). In contrast to Thomas et al. (2004), our results suggest that most of the respiratory CO_2 production occurred in the upper mixing layers of the water column, contributing to the CO_2 available for evasion to the atmosphere rather than export to the open sea.

CONCLUSION

Pronounced seasonal variability was observed, with higher rates of microplankton community respiration at the end of April, highest rates of bacterial production and bacterial growth efficiency in July, and lowest rates of CR_{O2}, BP and BGE in November. The relationship between microplankton community respiration and primary production differed between seasons, with ^{14}C-PP > CR_{O2} in April as a result of the phytoplankton bloom and ^{14}C-PP ~ CR_{O2} during July, due to the combination of lower ^{14}C-PP and higher CR_{O2}. Autotrophic and heterotrophic metabolic rates were driven by different environmental factors (temperature, nitrate+nitrite, DON and BA for the autotrophic metabolic rates, and nitrate+nitrite, DON, silicate, Chl-*a*, BA and ammonium for the heterotrophic metabolic rates) with different importance in the different months. Comparison of the upper mixing layer with the bottom mixing layer indicated a greater variability in community respiration and bacterial production in the UML despite similar concentrations of DOC and DON. However, bacterial respiration was similar in both layers. This constancy in the bacterial respiration rates might be explained by a lack of dependency of bacterial respiration on the production of dissolved organic carbon or / and by a difference in bacterial community composition. Our data clearly demonstrate that bacterial growth efficiency varies with season and depth as a response to the greater variability in bacterial production than respiration. Inclusion of this variability in BGE in future studies or model simulations is necessary for realistic carbon budget calculations as estimates of the production of CO_2 by bacteria derived using a constant BGE could incur significant biases.

Acknowledgements

We thank the captains and crew of the *RRS Discovery* for their help and support at sea and all the scientists involved in the three cruises. We would also like to thank Jo Hopkins and

748 Charlotte Williams (National Oceanographic Centre, Liverpool) for assistance and provision
749 of the physical characterization of the area, Malcolm Woodward and Carolyn Harris for
750 nutrient analyses, Clare Ostle and Jose Lozano for assistance on the dissolved oxygen
751 analysis (November cruise and April cruise, respectively), Callum White and Elaine Mitchel
752 for assistance on the bacterial production analysis (April cruise) and Ray Leakey for advice
753 on bacterial production methodology and data analysis. We are grateful to the UK Natural
754 Environment Research Council for funding the research cruises via the Shelf Sea
755 Biogeochemistry program. The data are publicly available under the NERC Open
756 Government Licence: http://www.bodc.ac.uk/data/documents/nodb/267802/

757 E.EG-M was funded by NERC grant NE/K00168X/1 (awarded to C. Robinson and D. A.
758 Purdie). SM, was funded by NERC grant NE/K001884/1 (awarded to K. Davidson). GAT
759 was funded by NERC grant NE/K002058/1. KMJM, AJP and CJD were funded by NERC
760 grant NE/K001701/1 (awarded to A.J. Poulton). CED and CM were funded by NERC grant
761 NE/K002007/1 (awarded to C. Mahaffey).

762

763 **REFERENCES**

764 Alonso-Sáez, L., Vázquez-Domínguez, E., Cardelús, C., Pinhassi, J., Sala, M., Lekunberri, I.,
765 Balagué, V., Vila-Costa, M., Unrein, F., Massana, R., Simó, R., Gasol, J. 2008. Factors
766 controlling the year-round variability in carbon flux through bacteria in a coastal marine
767 system. Ecosystems 11: 397-409.

768 Amin, S. A., Parker, M. S., Armbrust, E. V. 2012. Interactions between diatoms and bacteria.
769 Microbiology and Molecular Biology Reviews 76: 667-684.

770 Aranguren-Gassis, M., Teira, E., Serret, P., Martínez-García, S., Fernández, E. 2012.
771 Potential overestimation of bacterial respiration rates in oligotrophic plankton
772 communities. Marine Ecology Progress Series 453: 1-10.

773 Arbones, B., Castro, C. G., Alonso-Perez, F., Figueiras, F. G. 2008. Phytoplankton size
774 structure and water column metabolic balance in a coastal upwelling system: the Ría de
775 Vigo, NW Iberia. Aquatic Microbial Ecology 50: 169-179.

776 Baines, S. B., Pace, M. L. 1991. The production of dissolved organic matter by
777 phytoplankton and its importance to bacteria: patterns across marine and freshwater
778 systems. Limnology and Oceanography 36: 1078-1090.

779 Blight, S., Bentley, T., Lefevre, D., Robinson, C., Rodrigues, R., Rowlands, J., Williams, P.
780 J. leB. 1995. Phasing of autotrophic and heterotrophic plankton metabolism in a
781 temperate coastal ecosystem. Marine Ecology Progress Series 128: 61-75.

782 Brewer, P., Riley, J. 1965. The automatic determination of nitrate in sea water. Deep Sea
783 Research and Oceanographic Abstracts 12: 765-772.

784 Carlson, C. A., Hansell, D. A., Nelson, N. B., Siegel, D. A., Smethie, W. M., Khatiwala, S.,
785 Meyers, M. M., Halewood, E. 2010. Dissolved organic carbon export and subsequent
786 remineralization in the mesopelagic and bathypelagic realms of the North Atlantic basin.
787 Deep Sea Research Part II: Topical Studies in Oceanography 57: 1433-1445.

788 Carritt, D. E., Carpenter, J. H. 1966. Comparison and evaluation of currently employed
789 modifications of the Winkler method for determining dissolved oxygen in seawater; a
790 NASCO Report. Journal of Marine Research 24: 286-319.

791 Céa, B., Lefèvre, D., Chirurgien, L., Raimbault, P., Garcia, N., Charrière, B., Grégori, G.,
792 Ghiglione, J. F., Barani, A., Lafont, M., and Van Wambeke, F. 2014. An annual survey

of bacterial production, respiration and ectoenzyme activity in coastal NW Mediterranean waters: temperature and resource controls. Environmental Science and Pollution Research 22: 13654-13668.

Clarke, M. R. B. 1980. The reduced major axis of a bivariate sample. Biometrika 67: 441-446.

Cole, J. J. 1982. Interactions between bacteria and algae in aquatic ecosystems. Annual Review of Ecology and Systematics 13: 291-314.

Davidson, K., Gilpin, L. C., Pete, R., Brennan, D., McNeill, S., Moschonas, G., Sharples, J. 2013. Phytoplankton and bacterial distribution and productivity on and around Jones Bank in the Celtic Sea. Progress in Oceanography 117: 48-63.

Davis, C.E., Mahaffey, C., Wolf, G., Sharples, J. This issue. What's the matter: Seasonal organic matter dynamics across a temperate shelf sea. Progress in Oceanography.

De Haas, H., Van Weering, T. C., De Stigter, H. 2002. Organic carbon in shelf seas: sinks or sources, processes and products. Continental Shelf Research 22: 691-717.

Del Giorgio, P. A., Cole, J. J. 1998. Bacterial growth efficiency in natural aquatic systems. Annual Review of Ecology and Systematics: 503-541.

Del Giorgio, P. A., Cole, J. J. 2000. Bacterial energetics and growth efficiency, p. 289-325. Microbial ecology of the oceans. Wiley-Liss.

Del Giorgio, P. A., Gasol, J. M. 2008. Physiological structure and single-cell activity in marine bacterioplankton, p. 243-298. In D. L. Kirchman [ed.], Microbial Ecology of the Oceans. John Wiley & Sons, Inc.

814 Elser, J. J., Stabler, L. B., Hassett, R. P. 1995. Nutrient limitation of bacterial growth and
815 rates of bacterivory in lakes and oceans: a comparative study. Aquatic Microbial Ecology
816 9: 105-110.

817 García-Martín, Chris J. Daniels C. J., Davidson K., Lozano J., Mayers K. M. J., McNeill S.,
818 Mitchell E., Poulton A. J., Purdie D. A., Tarran G. A., Whyte C., Robinson C. This issue.
819 Plankton community respiration and bacterial metabolism in a North Atlantic Shelf Sea
820 during spring bloom development (April 2015). Progress in Oceanography.

821 Gasol, J. M., Morán, X. A. G. 1999. Effects of filtration on bacterial activity and
822 picoplankton community structure as assessed by flow cytometry. Aquatic Microbial
823 Ecology 16: 251-264.

824 Giering, S. L. C., Wells, S. R., Mayers, K. M. J., Tarran, G. A., Cornwell, L., Fileman, E.,
825 Atkinson, A., Mayor, D. J. This issue. Seasonal changes in zooplankton biomass,
826 community composition and stoichiometry in the UK Shelf Sea Progress in
827 Oceanography.

828 Gilbert, J. A., Field, D., Swift, P., Newbold, L., Oliver, A., Smyth, T., Somerfield, P. J.,
829 Huse, S., Joint, I. 2009. The seasonal structure of microbial communities in the Western
830 English Channel. Environmental microbiology 11: 3132-3139.

831 Gilbert, J. A., Steele, J. A., Caporaso, J. G., Steinbrück, L., Reeder, J., Temperton, B., Huse,
832 S., Mchardy, A. C., Knight, R., Joint, I. 2012. Defining seasonal marine microbial
833 community dynamics. The ISME Journal 6: 298-308.

834 Grasshoff, K., Kremling, K., Ehrhard, M. 1976. Methods of Seawater Analysis. 3rd
835 completely revised and extended edition. WILEY-VCH, Weinheim.

836 Griffith, P. C., Pomeroy, L. R. 1995. Seasonal and spatial variations in pelagic community
837 respiration on the southeastern US continental shelf. Continental Shelf Research 15: 815-
838 825.

839 Herndl, G. J., Reinthaler, T. 2013. Microbial control of the dark end of the biological pump.
840 Nature Geoscience 6: 718-724.

841 Hickman, A. E., Moore, C., Sharples, J., Lucas, M. I., Tilstone, G. H., Krivtsov, V., Holligan,
842 P. M. 2012. Primary production and nitrate uptake within the seasonal thermocline of a
843 stratified shelf sea. Marine Ecology Progress Series 463: 39-57.

844 Hickman A., Poulton, A.J., Mayers, K. M. J., Tarran, G. A. This issue. Seasonal variability in
845 size-fractionated chlorophyll-a and primary production in the Celtic Sea. Progress in
846 Oceanography.

847 Humphreys M. P., Moore, C. M., Achterberg E. P., Griffiths, A. M., Smilenova, A., Hartman
848 S. E., Kivimäe, C., Woodward, E.M.S. Hopkins, J. E. This issue. Balancing the inorganic
849 carbon and nutrient budgets in a seasonally-stratifying temperate shelf sea. Progress in
850 Oceanography.

851 Joint, I., Owens, N., Pomroy, A. 1986. Seasonal production of photosynthetic picoplankton
852 and nanoplankton in the Celtic Sea. Marine Ecology Progress Series 28: 251-258.

853 Joint, I., Pomroy, A. 1987. Activity of heterotrophic bacteria in the euphotic zone of the
854 Celtic Sea. Marine Ecology Progress Series 41: 155-165.

855 Joint, I., Wollast, R., Chou, L., Batten, S., Elskens, M., Edwards, E., Hirst, A., Burkill, P.,
856 Groom, S., Gibb, S. 2001. Pelagic production at the Celtic Sea shelf break. Deep Sea
857 Research Part II: Topical Studies in Oceanography 48: 3049-3081.

858 Kirchman, D. 2001. Measuring bacterial biomass production and growth rates from leucine
859 incorporation in natural aquatic environments. Methods in Microbiology 30: 227-237.

860 Kirchman, D. L. 2000. Uptake and regeneration of inorganic nutrients by marine
861 heterotrophic bacteria, p. 261-288. In D. L. Kirchman [ed.], Microbial Ecology of the
862 Oceans. Wiley.

863 Kirchman, D. L., Malmstrom, R. R., Cottrell, M. T. 2005. Control of bacterial growth by
864 temperature and organic matter in the Western Arctic. Deep-Sea Research Part II-Topical
865 Studies in Oceanography 52: 3386-3395.

866 Kirkwood, D. 1989. Simultaneous determination of selected nutrients in sea water.
867 International Council for the Exploration of the Sea (ICES).

868 Kritzberg, E. S., Duarte, C. M., Wassmann, P. 2010. Changes in Arctic marine bacterial
869 carbon metabolism in response to increasing temperature. Polar Biology. 33: 1673-1682.

870 La Ferla, R., Azzaro, M., Maimone, G. 2006. Microbial respiration and trophic regimes in the
871 Northern Adriatic Sea (Mediterranean Sea). Estuarine, Coastal and Shelf Science 69:
872 196-204.

873 Lee, C. W., Bong, C. W., Hii, Y. S. 2009. Temporal variation of bacterial respiration and
874 growth efficiency in tropical coastal waters. Applied and Environmental Microbiology
875 75: 7594-7601.

876 Legendre, L., Rivkin, R. B., Weinbauer, M. G., Guidi, L., Uitz, J. 2015. The microbial carbon
877 pump concept: potential biogeochemical significance in the globally changing ocean.
878 Progress in Oceanography 134: 432-450.

879 Legendre, P., Anderson, M. J. 1999. Distance-based redundancy analysis: testing
880 multispecies responses in multifactorial ecological experiments. Ecological Monographs
881 69: 1-24.

882 Lemée, R., Rochelle-Newall, E., Van Wambeke, F., Pizay, M. D., Rinaldi, P., Gattuso, J. P.
883 2002. Seasonal variation of bacterial production, respiration and growth efficiency in the
884 open NW Mediterranean Sea. Aquatic Microbial Ecology 29: 227-237.

885 Li, W., Dickie, P., Harrison, W., Irwin, B. 1993. Biomass and production of bacteria and
886 phytoplankton during the spring bloom in the western North Atlantic Ocean. Deep Sea
887 Research Part II: Topical Studies in Oceanography 40: 307-327.

888 Longnecker, K., Sherr, B., Sherr, E. 2006. Variation in cell-specific rates of leucine and
889 thymidine incorporation by marine bacteria with high and with low nucleic acid content
890 off the Oregon coast. Aquatic microbial ecology 43: 113-125.

891 López-Sandoval, D., Fernández, A., Marañón, E. 2011. Dissolved and particulate primary
892 production along a longitudinal gradient in the Mediterranean Sea. Biogeosciences 8:
893 815-825.

894 López-Urrutia, Á., and Morán, X. A. G. 2007. Resource limitation of bacterial production
895 distorts the temperature dependence of oceanic carbon cycling. Ecology 88: 817-822.

896 Maixandeau, A., Lefèvre, D., Fernández, I. C., Sempere, R., Sohrin, R., Ras, J., Van
897 Wambeke, F., Caniaux, G., Quéguiner, B. 2005. Mesoscale and seasonal variability of
898 community production and respiration in the surface waters of the NE Atlantic Ocean.
899 Deep-Sea Research Part I-Oceanographic Research Papers 52: 1663-1676.

900 Marra, J. 2002. Approaches to the measurement of plankton production, p. 78–108. In P. J.
901 leB. Williams, D. N. Thomas, and C. S. Reynolds [ed.], Phytoplankton Productivity:

902 Carbon Assimilation in Marine and Freshwater Ecosystems. Blackwell, Cambridge, U.
903 K.

904 Martin-Jézéquel, V., Videau, C. 1992. Phytoplankton and bacteria over the transient area of
905 the continental slope of the Celtic Sea in spring. I. Vertical distribution and productivity.
906 Marine Ecology Progress Series 85: 289-301.

907 Martínez-García, S., Fernández, E., Aranguren-Gassis, M., Teira, E. 2009. In vivo electron
908 transport system activity: a method to estimate respiration in natural marine microbial
909 planktonic communities. Limnology and Oceanography: methods 7: 459-469.

910 Mayers, K.M.J., Poulton, A.J., Daniels, C.J., Wells, S.R., Woodward, E.M.S., Tyrrell, T.,
911 Giering, S.L.C. This issue. Top-down control of coccolithophore populations during
912 spring in a temperate Shelf Sea (Celtic Sea, April 2015). Progress in Oceanography.

913 Miller, J. C., Miller, J. N. 1988. Statistics for analytical chemistry. 2nd Ed, Ellis Horwood,
914 Chichester.

915 Moore, C. M., Suggett, D. J., Hickman, A. E., Kim, Y.-N., Tweddle, J. F., Sharples, J.,
916 Geider, R. J., Holligan, P. M. 2006. Phytoplankton photoacclimation and
917 photoadaptation in response to environmental gradients in a shelf sea. Limnology and
918 Oceanography 51: 936-949.

919 Morán, X. A. G., Estrada, M., Gasol, J. M., Pedrós-Alió, C. 2002. Dissolved primary
920 production and the strength of phytoplankton– bacterioplankton coupling in contrasting
921 marine regions. Microbial Ecology 44: 217-223.

922 Pingree, R. D. 1980. Physical Oceanography of the Celtic Sea and English Channel, p. 415-
923 465. In M. B. C. F.T. Banner and K. S. Massie [eds.]. The North-West European Shelf
924 Seas: The Sea Bed and the Sea in Motion II. Physical and Chemical Oceanography, and
925 Physical Resources. Elsevier.

926 Pingree, R., Griffiths, D., Mardell, G. 1984. The structure of the internal tide at the Celtic Sea
927 shelf break. Journal of the Marine Biological Association of the United Kingdom 64: 99-
928 113.

929 Pomroy, A., Joint, I. 1999. Bacterioplankton activity in the surface waters of the Arabian Sea
930 during and after the 1994 SW monsoon. Deep Sea Research Part II: Topical Studies in
931 Oceanography 46: 767-794.

932 Poulton, A. J., Daniels, C. J., Esposito, M., Humphreys, M. P., Mitchell, E., Ribas-Ribas, M.,
933 Russell, B. C., Stinchcombe, M. C., Tynan, E., Richier, S. 2016. Production of dissolved
934 organic carbon by Arctic plankton communities: Responses to elevated carbon dioxide
935 and the availability of light and nutrients. Deep Sea Research Part II: Topical Studies in
936 Oceanography 127: 60-74.

937 Poulton, A.J., Davis, C.E., Daniels, C.J., Mayers, K.M.J., Harris, C., Tarran, G.A.,
938 Widdicombe, C.E., Woodward, E.M.S. This issue. Seasonal phosphorus dynamics in a
939 temperate shelf sea (Celtic Sea): uptake, release, turnover and stoichiometry. Progress in
940 Oceanography.

941 Reinthaler, T., Herndl, G. J. 2005. Seasonal dynamics of bacterial growth efficiencies in
942 relation to phytoplankton in the southern North Sea. Aquatic Microbial Ecology 39: 7-
943 16.

944 Rivkin, R. B., Anderson, M. R. 1997. Inorganic nutrient limitation of oceanic
945 bacterioplankton. Limnology and Oceanography 42: 730-740.

946 Robinson, C., Tilstone, G. H., Rees, A. P., Smyth, T. J., Fishwick, J. R., Tarran, G. A., Luz,
947 B., Barkan, E., David, E. 2009. Comparison of in vitro and in situ plankton production
948 determinations. Aquatic Microbial Ecology 54: 13-34.

949 Serret, P., Fernández, E., Sostres, J. A., Anadón, R. 1999. Seasonal compensation of
950 microbial production and respiration in a temperate sea. Marine Ecology Progress Series
951 187: 43-57.

952 Sharples, J., Mayor, D. J., Poulton, A. J., Rees, A. P., Robinson, C. This issue. Why do shelf
953 seas not run out of nutrients? Progress in Oceanography

954 Sharples, J., Moore, C. M., Hickman, A. E., Holligan, P. M., Tweddle, J. F., Palmer, M. R.,
955 Simpson, J. H. 2009. Internal tidal mixing as a control on continental margin ecosystems.
956 Geophysical Research Letters 36.

957 Sharples, J., Moore, M. C., Rippeth, T. P., Holligan, P. M., Hydes, D. J., Fisher, N. R.,
958 Simpson, J. H. 2001. Phytoplankton distribution and survival in the thermocline.
959 Limnology and Oceanography 46: 486-496.

960 Sherry, N. D., Boyd, P. W., Sugimoto, K., Harrison, P. J. 1999. Seasonal and spatial patterns
961 of heterotrophic bacterial production, respiration, and biomass in the subarctic NE
962 Pacific. Deep Sea Research Part II: Topical Studies in Oceanography 46: 2557-2578.

963 Sintes, E., Stoderegger, K., Parada, V., Herndl, G. J. 2010. Seasonal dynamics of dissolved
964 organic matter and microbial activity in the coastal North Sea. Aquatic Microbial
965 Ecology 60: 85.

966 Tarran, G. A., Hickman, A. E., Poulton, A. J., Widdicombe, C. E., Rees, A. P., Fox, J. E.,
967 Munns, L. This issue. European Shelf Sea phyto- and microplankton: communities,
968 abundance and seasonality in the Celtic Sea. Progress in Oceanography.

969 Thomas, H., Bozec, Y., Elkalay, K., De Baar, H. J. 2004. Enhanced open ocean storage of
970 CO_2 from shelf sea pumping. Science 304: 1005-1008.

971 Vázquez-Domínguez, E., Vaqué, D., Gasol, J. M. 2007. Ocean warming enhances respiration
972 and carbon demand of coastal microbial plankton. Global Change Biology 13: 1327-
973 1334.

974 Wihsgott J. U., Sharples J., Hopkins J. E., Woodward E. M. S., Greenwood N., Hull T.,
975 Sivyer D. B. This issue. Investigating the autumn bloom's significance within the
976 seasonal cycle of primary production in a temperate shelf sea. Progress in Oceanography.
977 *In rev*.

978

979

980 Table 1. Average surface ± standard error environmental conditions and the depth of the base
981 of the thermocline at the Central Celtic Sea (CCS) and Shelf Edge (CS2) stations in
982 November 2014, April 2015 and July 2015. * indicates there was only one datum for the
983 analysis.

	November 2014		April 2015		July 2015	
	CCS	CS2	CCS	CS2	CCS	CS2
SST (˚C)	13.3 ± 0.18	14.01 ± 0.13	10.49 ± 0.2	11.5 ± 0.15	16.46 ± 0.22	16 *
Salinity	35.39 ± 0.01	35.57 ± 0.01	35.33 ± 0.01	35.59 ± 0.01	35.42 ± 0.02	35.54 *
Nitrate+nitrite (µM)	2.11 ± 0.14	3.03 ± 0.46	3.19 ±0.95	7.16 ± 1.06	<0.02	<0.02 *
Ammonium (µM)	0.14 ± 0.02	9.09 ± 0.01	0.10 ±0.02	0.09 ± 0.05	0.06 *	0.1 *
Phosphate (µM)	0.19 ± 0.01	0.25 ± 0.03	0.30 ± 0.06	0.45 ± 0.06	0.07 ± 0.01	0.07 *
Silicate (µM)	0.93 ± 0.06	1.35 ± 0.04	2.55 ± 0.08	2.73 ± 0.4	0.36 ± 0.17	0.2 *
Chlorophyll-a (µg L^{-1})	1.53 ± 0.09	0.84	3.51 ±0.92	1.55 ± 0.72	0.29 ± 0.02	0.92 *
Bacterial abundance (x10^6 cells mL^{-1})	0.7 ± 0.1	0.5 ± 0.1	1.0 ± 0.1	0.5 ± 0.1	0.8 ± 0.1	1.4 *
Thermocline (m)	75 ± 7	114 ± 5	54 ± 4	67 ± 2	53 ± 2	50 *

984

985

Table 2. Upper mixing layer depth integrated bacterial carbon demand (BCD), bacterial growth efficiency (BGE), cell-specific bacterial respiration ($INT_{0.2-0.8}$) and cell-specific bacterial production (BP) ± standard errors during November, April and July at CCS and CS2.

Station	Date	BCD	BGE	cell-specific $INT_{0.2-0.8}$	cell-specific BP
		mg C m^{-2} d^{-1}	%	fmol O_2 $cell^{-1}$ d^{-1}	fmol C $cell^{-1}$ d^{-1}
CCS	10/11/2014	23.4 ± 2.3	33.2 ± 3.5	0.42 ± 0.06	0.21 ± 0.01
	12/11/2014	23.7 ± 2	18.4 ± 1.5		
	22/11/2014	24.1 ± 1.1	34.8 ± 1.6	0.32 ± 0.02	0.17 ± 0
	25/11/2014	27.8 ± 2.2	24.4 ± 2.1	0.34 ± 0.04	0.11 ± 0
CS2	18/11/2014	23.6 ± 3.3	22.9 ± 3.3	0.41 ± 0.07	0.12 ± 0
CCS	04/04/2015	30.8 ± 4.7	24.9 ± 4.7	0.46 ± 0.09	0.15 ± 0.02
	06/04/2015				
	11/04/2015	24.2 ± 2.3	50.5 ± 5.4	0.23 ± 0.04	0.24 ± 0.01
	15/04/2015	44.5 ± 2.9	28.7 ± 2.1	0.51 ± 0.05	0.20 ± 0.01
	20/04/2015	32.1 ± 2.1	48 ± 4.3	0.23 ± 0.03	0.21 ± 0.01
	25/04/2015	27 ± 0.8	45.8 ± 1.8	0.44 ± 0.02	0.37 ± 0.01
CS2	10/04/2015	25.3 ± 2.7	18.1 ± 2.1	0.89 ± 0.11	0.20 ± 0.01
	24/04/2015	21.8 ± 5.4	35.7 ± 9	0.36 ± 0.14	0.20 ± 0.01
CCS	14/07/2015	25.5 ± 1.9	62.5 ± 4.8	0.2 ± 0.04	0.33 ± 0
	24/07/2015	23.5 ± 1.2	70.6 ± 3.9	0.14 ± 0.02	0.33 ± 0.01
	29/07/2015	21.4 ± 1.5	55.6 ± 3.9	0.25 ± 0.04	0.31 ± 0
CS2	19/07/2015	24.7 ± 1.4	57.3 ± 3.5	0.23 ± 0.03	0.31 ± 0.01

Table 3. Spearman correlation matrix between volumetric bacterial abundance (BA), microplankton community respiration (CR_{O2}, and INT_T), bacterial respiration ($INT_{0.2-0.8}$), bacterial production (BP), bacterial carbon demand (BCD) and bacterial growth efficiency (BGE) with environmental parameters (temperature, T; chlorophyll-*a*, Chl-*a*; nitrate+nitrite, ammonium, silicate and phosphate concentration and phytoplankton DOC production, *p*DOC).

	T	**Chl-*a***	**Nitrate +nitrite**	**Ammonium**	**Silicate**	**Phosphate**	***p*DOC**	**CR_{O2}**	**INT_T**	**INT_{02-08}**	**%INT_{02-08}**	**BP**	**BCD**
BA	**-0.57** **	**0.38** **	**-0.42** ***	0.50	-0.11	**-0.32** **	**0.49** **	**0.48** ***	**0.72** ***	**0.28** **	**-0.47** ***	**0.67** ***	**0.62** ***
CR_{O2}	-0.04	**0.40** ***	**-0.32** **	0.17	-0.12	**-0.40** ***	**0.53** ***		**0.62** ***	0.17	**-0.48** ***	**0.75** ***	**0.60** ***
INT_T	**-0.36** ***	**0.54** ***	**-0.39** ***	0.05	0.01	**-0.26** *	**0.64** ***	**0.62** ***		**0.55** ***	**-0.45** ***	**0.63** ***	**0.79** ***
INT_{02-08}	**-0.42** ***	**0.38** ***	-0.12	0.01	**0.21** *	0.09	0.13	0.17	**0.55** ***		**0.40** ***	0.12	**0.75** ***
%INT_{02-08}	-0.04	-0.21	**0.31** ***	-0.10	0.14	**0.34** **	**-0.62** ***	**-0.48** ***	**-0.45** ***	**0.40** ***		**-0.51** ***	-0.06
BP	0.15	**0.34** **	**-0.68** ***	**0.35** ***	**-0.48** ***	**-0.69** ***	**0.59** ***	**0.75** ***	**0.63** ***	0.12	**-0.51** ***		**0.70** ***
BCD	-0.19	**0.42** ***	-0.12	0.16	-0.13	**-0.36** ***	**0.47** **	**0.60** ***	**0.79** ***	**0.75** ***	-0.06	**0.70** ***	
BGE	**0.37** ***	-0.04	**-0.53** ***	**0.30** ***	**-0.51** ***	**-0.64** ***	**0.43** **	**0.52** ***	**0.22** *	**-0.48** ***	**-0.75** ***	**0.75** ***	0.16

LEGEND

Figure 1. Time course of the temperature vertical distribution in the upper 130 m at CCS and CS2 during November 2014, April 2015 and July 2015. Black dots represent the depths where water was collected for measurement of plankton metabolic rates and the dotted white line is the base of the thermocline considered to be the base of the upper mixing layer.

Figure 2. Paired measurements of log-transformed microplankton community respiration derived from 24h oxygen consumption (CR_{O2}) and <1.5 h INT reduction rates (INT_T) determined from samples collected at CCS and CS2. The different colours correspond to the different months sampled: November in blue, April in green and July in orange. The dashed line corresponds to the ordinary least-squares linear relationship. The statistical Spearman correlation analysis is shown.

Figure 3. Vertical profiles of the monthly average bacterial abundance (BA), microplankton community respiration (CR_{O2} and INT_T), respiration of the plankton fraction >0.8 µm ($INT_{>0.8}$), bacterial respiration ($INT_{0.2\text{-}0.8}$) and bacterial production (BP) at CCS (A, B, C, D, E, F) and CS2 (G, H, I, J, K, L) in November 2014 (blue), April 2015 (green) and July 2015 (orange). Error bars represent the standard error of the averages.

Figure 4. Upper mixing layer depth-integrated bacterial abundance (BA), microplankton community respiration (CR_{O2}), bacterial respiration ($INT_{0.2\text{-}0.8}$), proportion of plankton community respiration attributable to bacteria (%$INT_{0.2\text{-}0.8}$) and bacterial production (BP) at CCS (solid circles) and CS2 (open circles) during November 2014 (blue), April 2015 (green) and July 2015 (orange). Error bars represent the standard error.

Figure 5. Volumetric bacterial carbon demand (BCD) versus dissolved organic carbon produced as a result of phytoplankton photosynthesis (*p*DOC) during November 2014 (blue), April 2015 (green) and July 2015 (orange). The straight line is the 1:1 line.

Figure 6. Relationship between depth-integrated microplankton community respiration (CR_{O2}), bacterial production (BP), bacterial respiration ($INT_{0.2-0.8}$), contribution of bacteria to microplankton respiration ($\%INT_{0.2-0.8}$) and bacterial growth efficiency (BGE) with dissolved organic carbon (DOC) and nitrogen (DON).

Figure 7. Distance-based redundancy analysis (dbRDA) of the linear model describing the relationships between environmental variables (temperature, T; nitrate+nitrite concentration; silicate concentration; ammonium concentration, bacterial abundance, BA; chlorophyll-*a*, Chl-*a*; dissolved organic nitrogen, DON) and (A) autotrophic metabolic rates (primary production and production of dissolved organic carbon) and (B) heterotrophic metabolic rates (daily microbial respiration, respiration of the >0.8 µm size fraction, bacterial respiration, bacterial production and bacterial growth efficiencies). Sampling days at CCS are represented by triangles and at CS2 by circles in November (blue), April (green) and July (orange). Significant environmental variables explaining the variability of the ordination (best selection procedure) are represented by the lines.

Figure 8. Weighted average (depth-integrated rate divided by the depth of integration) microplankton community respiration (CR_{O2}), bacterial respiration ($INT_{0.2-0.8}$), percentage microplankton community respiration attributable to bacteria ($\%INT_{0.2-0.8}$), bacterial production (BP), cell-specific bacterial respiration and cell-specific bacterial production in the upper mixing layer (UML, solid circles) and bottom mixing layer (BML, open circles) at CCS (A, C, E, G, I and K) and CS2 (B, D, F, H, J, L) in November, April and July.

Figure 9. Daily microplankton community respiration (CR_{O2}) versus primary production determined from radiolabelled bicarbonate uptake after a 6-8 h incubation (^{14}C-PP) in November 2014 (blue), April 2015 (green) and July 2015 (orange) (A). (B) Zoom of the

dotted area in (A) with November and April data only. Error bar represents the standard error and the solid line is the 1:1 line.

Figure 1.

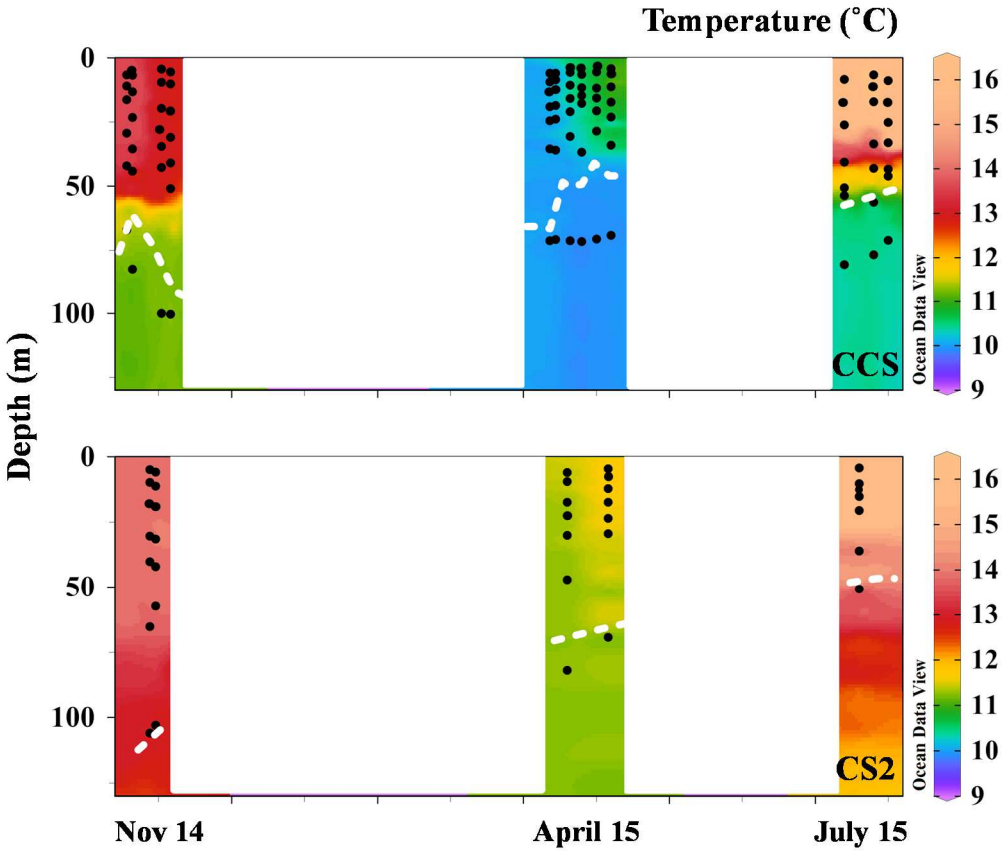
Temperature (°C)
Depth (m)
0
50
100
CCS
CS2
Ocean Data View
16
15
14
13
12
11
10
9
Nov 14
April 15
July 15

Figure 2.

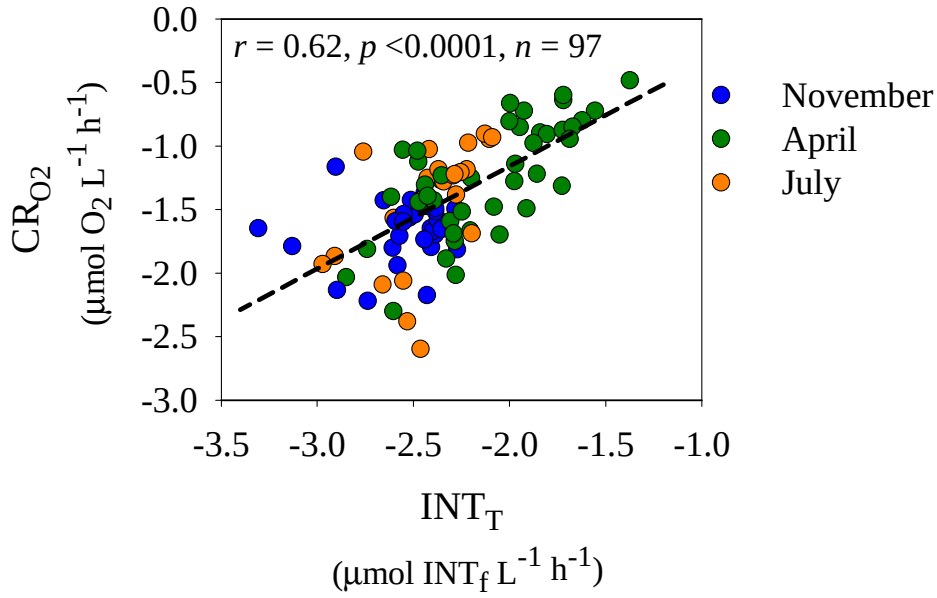
r = 0.62, p <0.0001, n = 97
0.0
-0.5
-1.0
-1.5
-2.0
-2.5
-3.0
-3.5
-3.0
-2.5
-2.0
-1.5
-1.0
CR$_{O2}$ (µmol O$_2$ L^{-1} h^{-1})
INT$_T$
(µmol INT$_f$ L^{-1} h^{-1})
November
April
July

Figure 3.

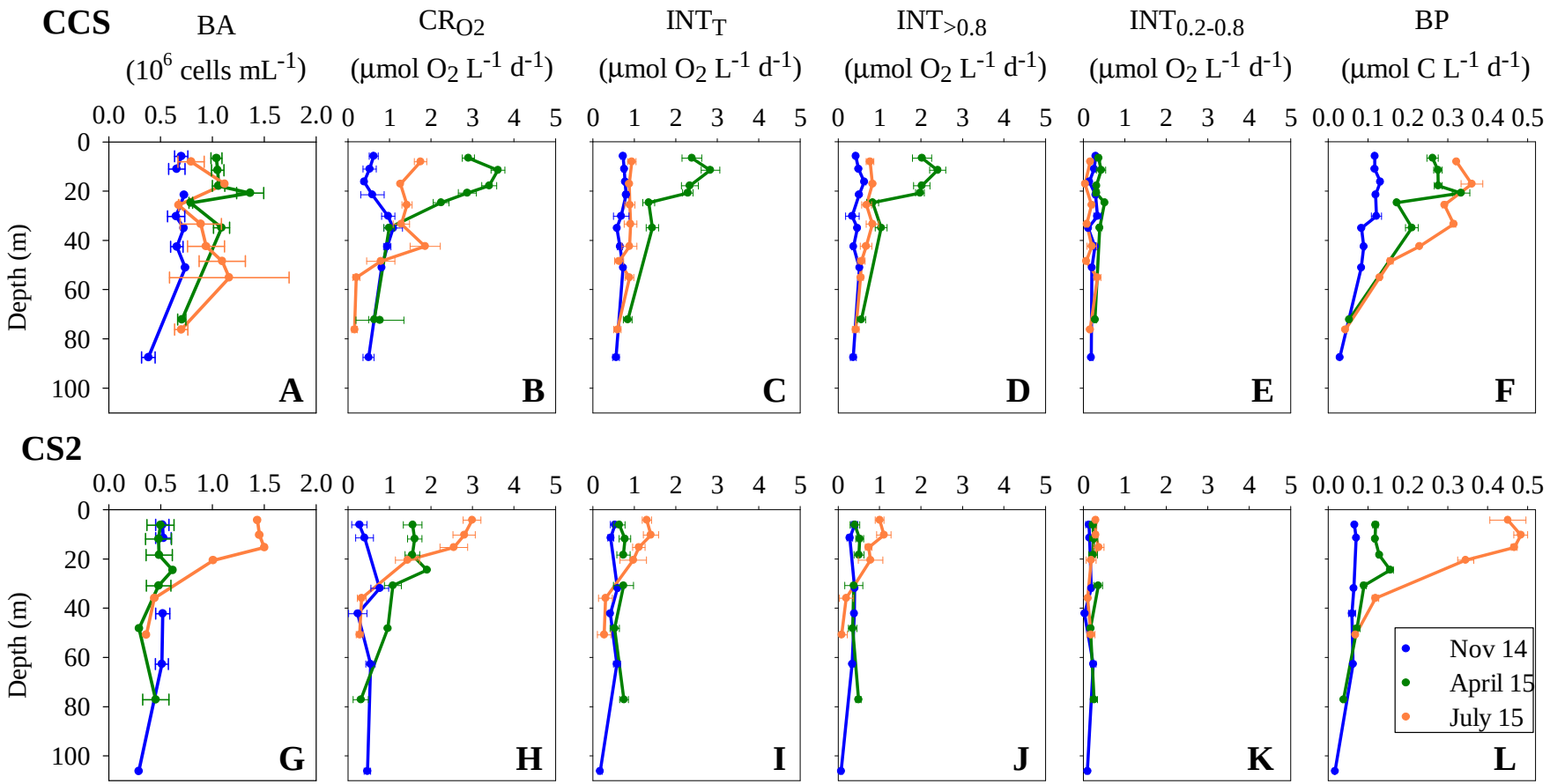
CCS
BA
(10^6 cells mL^{-1})
CR_{O2}
(µmol O_2 L^{-1} d^{-1})
INT_T
(µmol O_2 L^{-1} d^{-1})
$INT_{>0.8}$
(µmol O_2 L^{-1} d^{-1})
$INT_{0.2-0.8}$
(µmol O_2 L^{-1} d^{-1})
BP
(µmol C L^{-1} d^{-1})
Depth (m)
A
B
C
D
E
F
CS2
G
H
I
J
K
L
Nov 14
April 15
July 15

3 Figure 4.

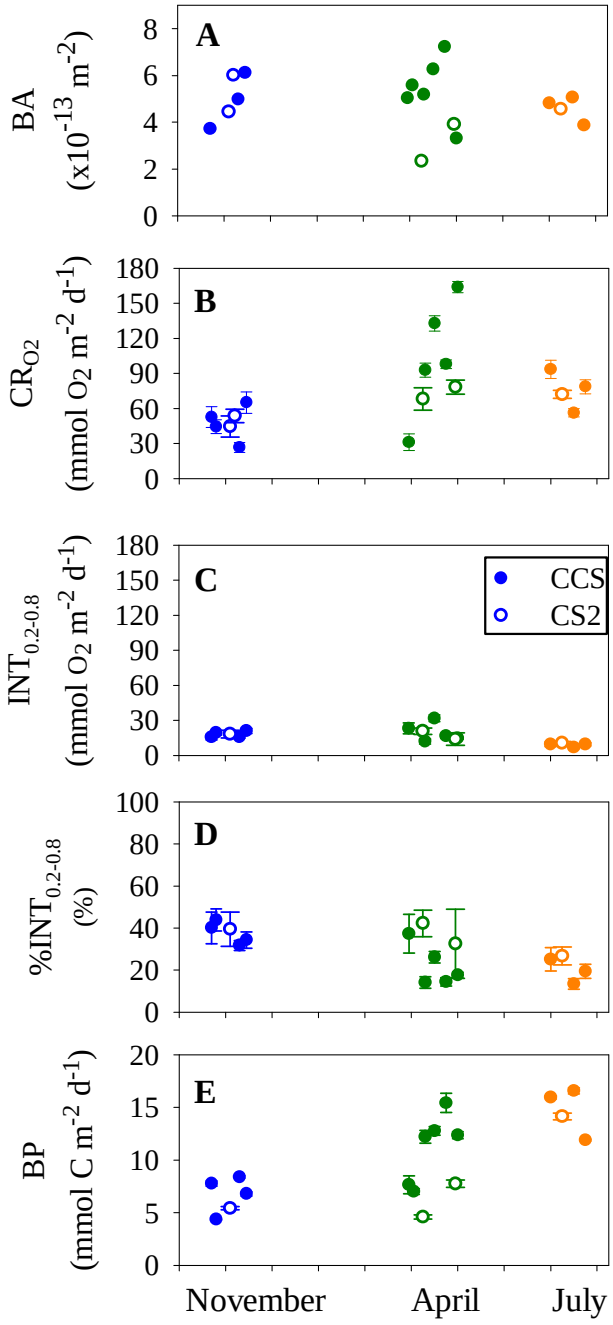
A
BA
(x10-13 m-2)
8
6
4
2
0
B
CRO2
(mmol O2 m-2 d-1)
180
150
120
90
60
30
0
C
INT0.2-0.8
(mmol O2 m-2 d-1)
CCS
CS2
D
%INT0.2-0.8
(%)
100
80
60
40
20
0
E
BP
(mmol C m-2 d-1)
20
15
10
5
0
November
April
July

Figure 5.

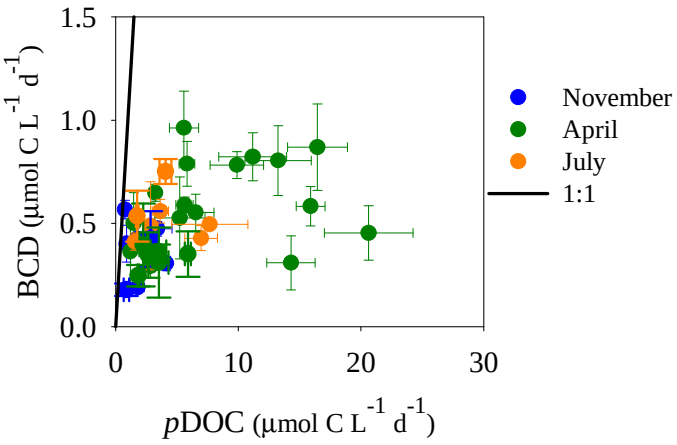
1.5
1.0
0.5
0.0
BCD (µmol C L-1 d-1)
0
10
20
30
pDOC (µmol C L-1 d-1)
November
April
July
1:1

6 Figure 6.

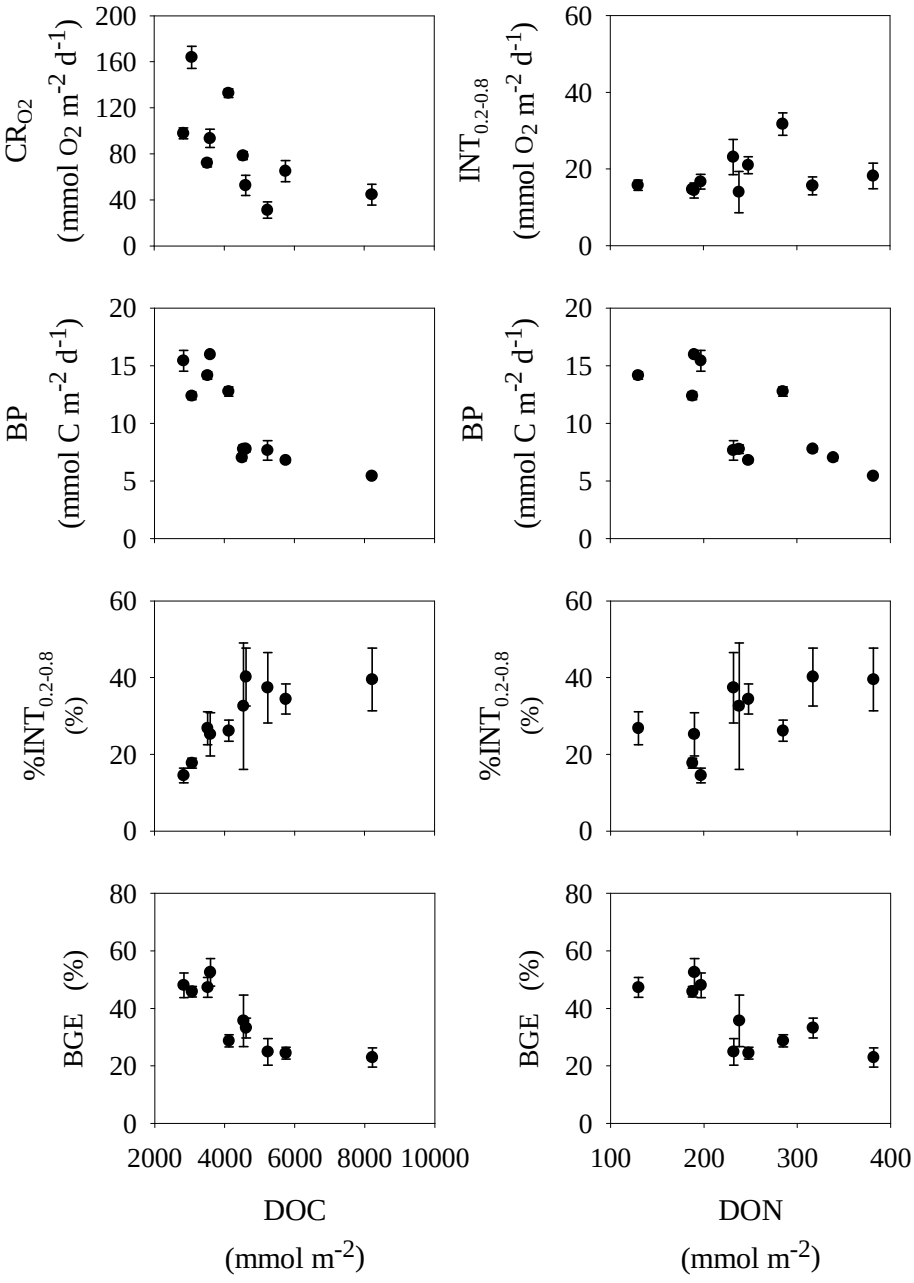
CR$_{O2}$ (mmol O$_2$ m^{-2} d^{-1})
INT$_{0.2-0.8}$ (mmol O$_2$ m^{-2} d^{-1})
BP (mmol C m^{-2} d^{-1})
BP (mmol C m^{-2} d^{-1})
%INT$_{0.2-0.8}$ (%)
%INT$_{0.2-0.8}$ (%)
BGE (%)
BGE (%)
DOC (mmol m^{-2})
DON (mmol m^{-2})

7

8 Figure 7.

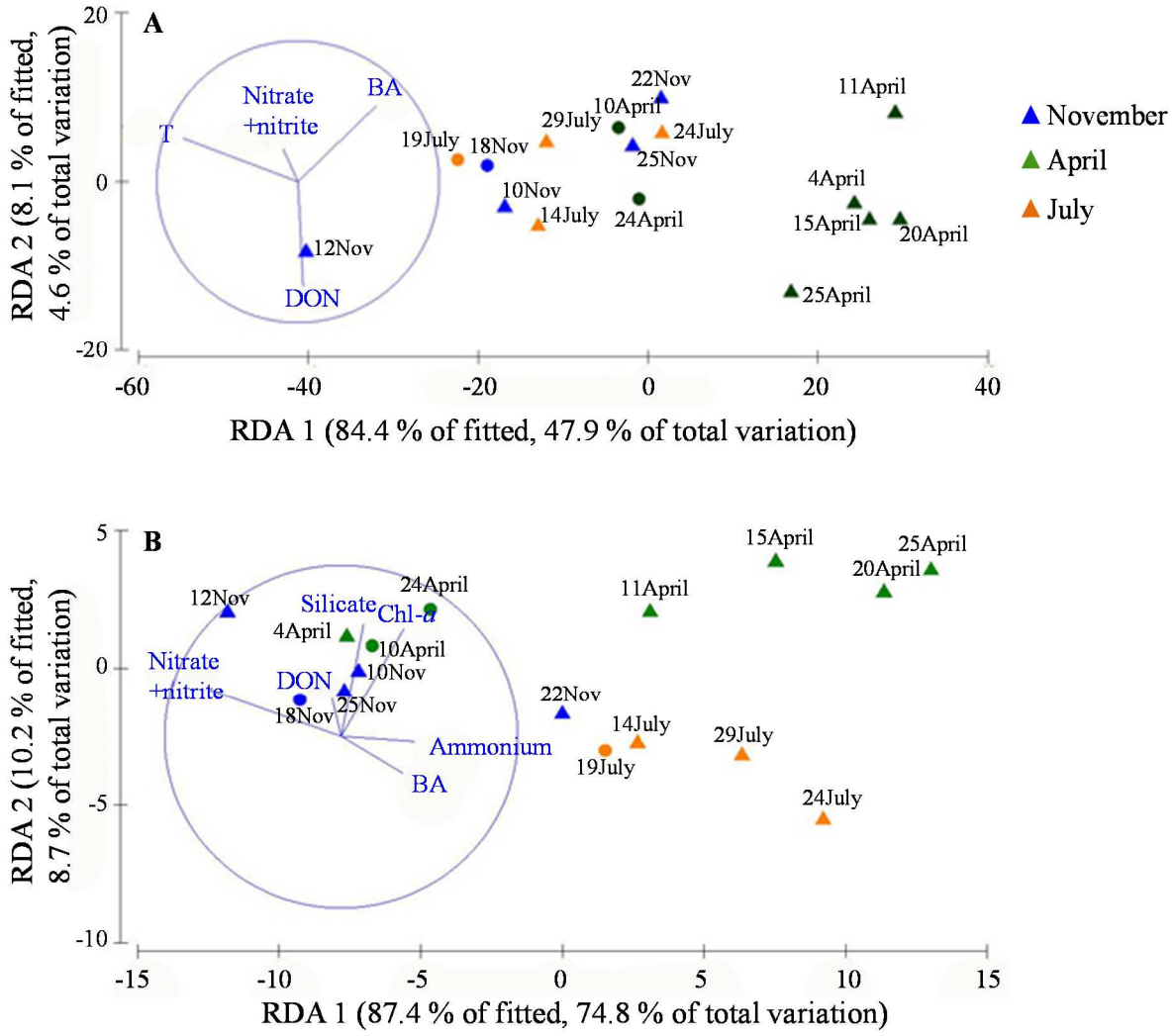
A
RDA 2 (8.1 % of fitted, 4.6 % of total variation)
RDA 1 (84.4 % of fitted, 47.9 % of total variation)
Nitrate +nitrite
BA
T
DON
12Nov
10Nov
18Nov
19July
29July
14July
22Nov
10April
24July
25Nov
24April
11April
4April
15April
20April
25April
November
April
July
B
RDA 2 (10.2 % of fitted, 8.7 % of total variation)
RDA 1 (87.4 % of fitted, 74.8 % of total variation)
Silicate
Chl-a
Nitrate +nitrite
DON
BA
Ammonium
12Nov
24April
4April
10April
10Nov
25Nov
18Nov
22Nov
14July
19July
29July
24July
11April
15April
25April
20April

9

10 Figure 8.

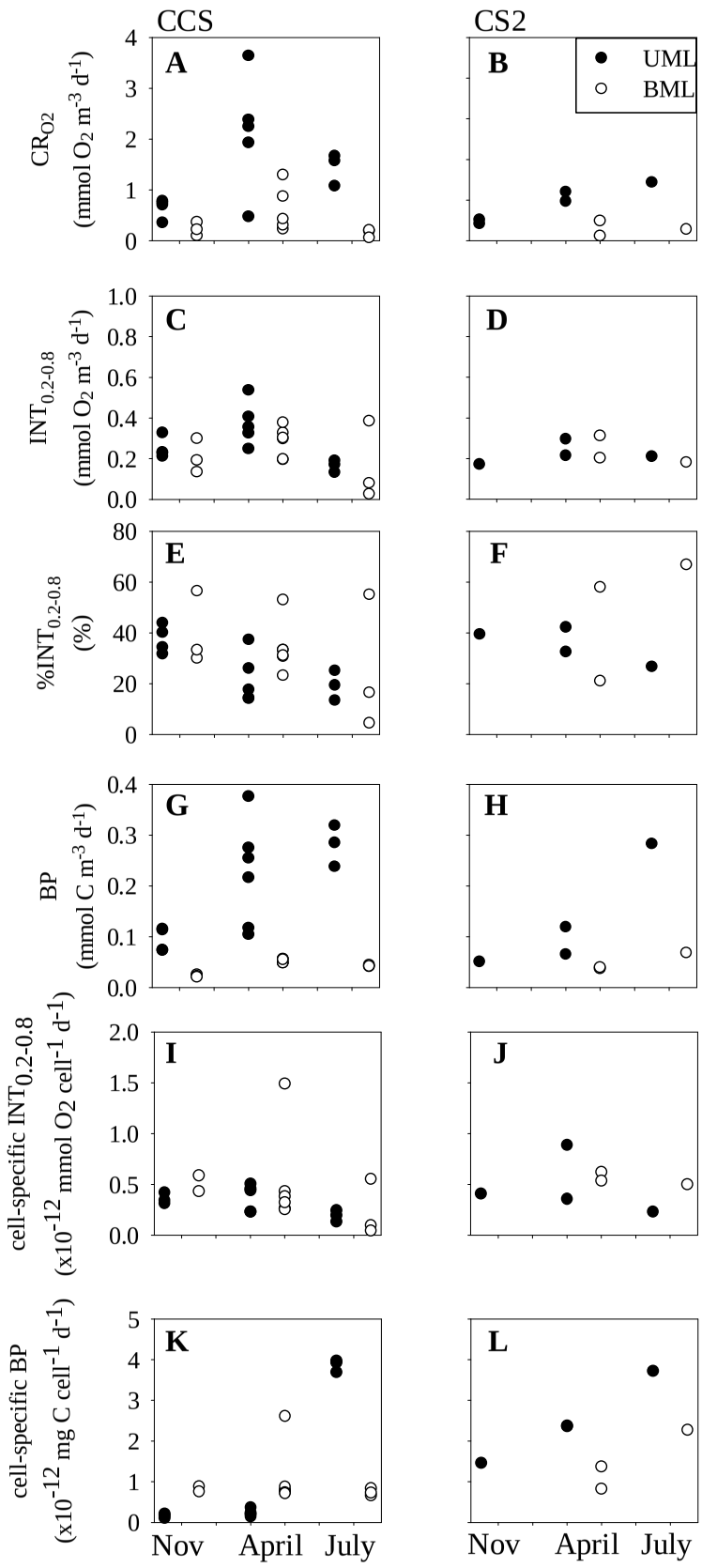
CCS
CS2
A
B
C
D
E
F
G
H
I
J
K
L
UML
BML
CR_{O2} (mmol O_2 m^{-3} d^{-1})
$INT_{0.2-0.8}$ (mmol O_2 m^{-3} d^{-1})
$\%INT_{0.2-0.8}$ (%)
BP (mmol C m^{-3} d^{-1})
cell-specific $INT_{0.2-0.8}$ ($x10^{-12}$ mmol O_2 $cell^{-1}$ d^{-1})
cell-specific BP ($x10^{-12}$ mg C $cell^{-1}$ d^{-1})
Nov
April
July

Figure 9.

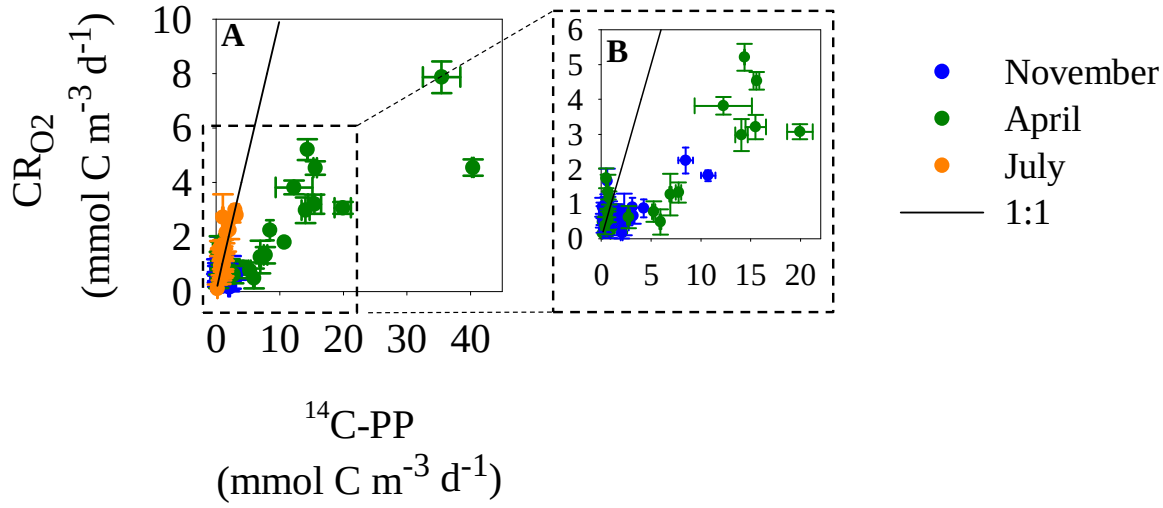

Supplementary Table 1. Volumetric and depth-integrated rates of microplankton community respiration, (CR); bacterial production, (BP), bacterial respiration, (BR); bacterial carbon demand, (BCD); and bacterial growth efficiency, (BGE) in temperate Shelf Seas.

Publication	Site	Variable	Period	Value	Units
Blight et al. 1995	Liverpool Bay	CR	Seasonal	<2	mmol O_2 m^{-3} d^{-1}
Serret et al. 1999	Bay of Biscay	CR	Seasonal	1 - 9	mmol O_2 m^{-3} d^{-1}
Céa et al. 2014	Mediterranean	CR	Seasonal	0 - 6.46	mmol O_2 m^{-3} d^{-1}
Serret et al. 1999	Bay of Biscay	integrated CR	Seasonal	10 - 180	mmol O_2 m^{-2} d^{-1}
Arbones et al. 2008	Ria de Vigo	integrated CR	April	104.5	mmol O_2 m^{-2} d^{-1}
Arbones et al. 2008	Ria de Vigo	integrated CR	July	74.5	mmol O_2 m^{-2} d^{-1}
Arbones et al. 2008	Ria de Vigo	integrated CR	October	30	mmol O_2 m^{-2} d^{-1}
Robinson 2009	Celtic Sea	integrated CR	April	17 - 73	mmol O_2 m^{-2} d^{-1}
This study	Celtic Sea	CR	November	0.1- 1.6	mmol O_2 m^{-3} d^{-1}
This study	Celtic Sea	CR	April	0.1 - 7.9	mmol O_2 m^{-3} d^{-1}
This study	Celtic Sea	CR	July	0.1 - 3.0	mmol O_2 m^{-3} d^{-1}
This study	Celtic Sea	integrated CR	Seasonal	27 - 164	mmol O_2 m^{-2} d^{-1}
Alonso-Saez et al. 2008	Bay of Biscay	BR	Seasonal	0.4 - 5.8	mmol C m^{-3} d^{-1}
Reinthaler & Herndl 2005	North Sea	BR	Seasonal	0.2 - 7	mmol C m^{-3} d^{-1}
Lemee et al. 2002	Mediterranean	BR	Seasonal	0.05 - 2	mmol O_2 m^{-3} d^{-1}
This study	Celtic Sea	BR	November	0.05 - 0.49	mmol O_2 m^{-3} d^{-1}
This study	Celtic Sea	BR	April	0.07 - 0.85	mmol O_2 m^{-3} d^{-1}
This study	Celtic Sea	BR	July	0.03 - 0.39	mmol O_2 m^{-3} d^{-1}
This study	Celtic Sea	integrated BR	Seasonal	7 - 32	mmol O_2 m^{-2} d^{-1}
Martin-Jezequel & Videau 1992	Celtic Sea	BP	April	<0.2 - 0.4	mg C m^{-3} d^{-1}
Davidson et al. 2013	Celtic Sea	BP	July	2 -25	mg C m^{-3} d^{-1}
Davidson et al. 2013	Celtic Sea	integrated BP	July	420 - 700	mg C m^{-2} d^{-1}
Lemee et al. 2002	Mediterranean	BP	Seasonal	0.6 - 3	mg C m^{-3} d^{-1}
Alonso-Saez et al. 2008	Bay of Biscay	BP	Seasonal	< 1 - 6	mg C m^{-3} d^{-1}
Reinthaler & Herndl 2005	North Sea	BP	Seasonal	0.1 - 24	mg C m^{-3} d^{-1}
Céa et al. 2014	Mediterranean	BP	Seasonal	0 - 4.8	mg C m^{-3} d^{-1}
Joint & pomeroy 1987	Celtic Sea	integrated BP	Seasonal	1 - 24.5	mg C m^{-2} d^{-1}
This study	Celtic Sea	BP	November	0.2 - 1.9	mg C m^{-3} d^{-1}
This study	Celtic Sea	BP	April	0.4 - 5.0	mg C m^{-3} d^{-1}
This study	Celtic Sea	BP	July	0.5 - 5.8	mg C m^{-3} d^{-1}
This study	Celtic Sea	integrated BP	Seasonal	52 - 199	mg C m^{-2} d^{-1}
Joint et al. 2001	Celtic Sea	integrated BCD	November	50	mg C m^{-2} d^{-1}
Joint et al. 2001	Celtic Sea	integrated BCD	April	100 - 150	mg C m^{-2} d^{-1}
Joint et al. 2001	Celtic Sea	integrated BCD	July	100 - 130	mg C m^{-2} d^{-1}
This study	Celtic Sea	integrated BCD	November	281 - 333	mg C m^{-2} d^{-1}
This study	Celtic Sea	integrated BCD	April	261 - 534	mg C m^{-2} d^{-1}
This study	Celtic Sea	integrated BCD	July	257 - 306	mg C m^{-2} d^{-1}
Sintes et al. 2010	North Sea	BGE	Seasonal	3 - 71	%
Reinthaler & Herndl 2005	North Sea	BGE	Seasonal	5 - 28	%
Lemee et al. 2002	Mediterranean	BGE	Seasonal	5 - 45	%
Céa et al. 2014	Mediterranean	BGE	Seasonal	1 - 37	%
Alonso-Saez et al. 2008	Bay of Biscay	BGE	Seasonal	2 - 30	%
Robinson et al. 2002	North Sea	BGE	June-July	18	%
This study	Celtic Sea	BGE	November	18 - 33	%
This study	Celtic Sea	BGE	April	18 - 51	%
This study	Celtic Sea	BGE	July	56 - 71	%